Research Square

Preprints are preliminary reports that have not undergone peer review.
They should not be considered conclusive, used to inform clinical practice,
or referenced by the media as validated information.

Sediment, solution, plant: decomposing the caesium transfer factor in Styrian ponds after Chernobyl

Gilbert Ahamer

gilbert.ahamer@uni-graz.at

Research Article

Keywords: Radiocaesium, Potassium-40, Transfer factor, Sediment desorption, Aquatic plants, Chernobyl

Posted Date: November 24th, 2026

DOI: https://doi.org/10.21203/rs.3.rs-11641038/v1

License: This work is licensed under a Creative Commons Attribution 4.0 International License.
Read Full License

Additional Declarations: No competing interests reported.

Sediment, solution, plant: decomposing the caesium transfer factor in Styrian ponds after Chernobyl

Gilbert Ahamer
Global Studies, University of Graz, Austria
Correspondence: Macherstrasse 15, 8047 Graz, Austria
E-mail: gilbert.ahamer@uni-graz.at
ORCID: 0000-0003-2140-7654

Abstract

Using the original files of a 1987 survey of 26 Styrian water bodies, the sediment-to-plant transfer factor (TF) of radiocaesium was split into a solution factor (desorbed/sediment activity) and a nutrition factor (plant/desorbed activity). Potassium was desorbed eight times more readily than caesium, whereas uptake from solution did not differ detectably. The decline of TF with contamination, also found for Chernobyl-derived ^{134}Cs, resided mainly in the desorption step, but only if weak solution values are unbiased. Whether weapons-test caesium was less available than Chernobyl caesium cannot be decided. Targeted laboratory tests are needed.

Article Highlights

- Caesium transfer from pond sediment to plants was split into a desorption step and an uptake step.
- Potassium was desorbed eight times more readily than caesium; uptake from solution did not differ detectably.
- Transfer declined with contamination also for Chernobyl ^{134}Cs, mainly in desorption if weak values are unbiased.

Keywords: Radiocaesium; Potassium-40; Transfer factor; Sediment desorption; Aquatic plants; Chernobyl

1. Introduction

The transfer factor TF = C_{plant} / $C_{substrate}$ (both on a dry-weight basis) is the standard coefficient of radioecological assessment [1]. Its values for caesium scatter over several orders of magnitude [1–3]. Part of this scatter arises because a single ratio combines two processes that different parts of the system control. Caesium must first pass from the solid phase into the soil or pore solution; the plant then takes it up through its potassium transport systems [4, 5]. The first step depends on the selective sorption of caesium on frayed-edge and interlayer sites of micaceous clay minerals and on the potassium and ammonium that compete for them [6–11]. In

freshwater sediments, ^{137}Cs is held preferentially by micaceous minerals [12], and its exchange with the pore water controls its remobilisation in lakes and reservoirs [13–15]; the behaviour of Chernobyl radiocaesium in lakes and their catchments has been reviewed by Smith and Beresford [16]. The second step depends on the plant and on the potassium status of the solution [17].

The link between the exchangeable fraction of caesium and its availability to plants was recognised early [18, 19]. Desorption tests with salt solutions were applied to estuarine silts and to Chernobyl-contaminated soils [20, 21], and Sheppard [22] examined the correlation between solid–liquid partitioning coefficients and plant concentrations. Studies that related the bioavailability of ^{137}Cs to the properties of many soils found large variations of the transfer coefficients that soil parameters explained only in part [23, 24]. Models that predict TF from the solid–liquid distribution coefficient and the potassium in solution explain much of the variation between soils [17, 25–27]. Most of this knowledge comes from pot experiments with homogenised soils. Field data in which the solution step was measured directly at many sites are rare, particularly for aquatic systems.

A survey of 26 Styrian water bodies in 1987 provides such data [28–32]. Its design accepted the heterogeneity of real sites and species instead of controlling it, because an assessment of actual exposure must include influences that pot experiments exclude [30, Section 2.1]. The large variability of the biospheric conditions was intended, so that the data reflect real-life conditions; it also limits how closely the quantities can be correlated and modelled. The project report therefore called its model preliminary, to be improved by targeted laboratory tests of the most important parameters, and hoped to have gone a step beyond the publication of mere "number cemeteries" [30, p. 7]. A re-examination of the transfer factors (Ahamer, submitted to J. Environ. Radioact.) found that TF declined with sediment activity with an exponent of about –0.5. Part of this decline is explained by ratio arithmetic and sampling error, and the re-examination located the remaining sub-proportionality most plausibly in the partitioning of caesium between sediment and water. The mineralogy and depth profiles are described separately (Ahamer, submitted to Nucl. Eng. Technol.), and the database by Ahamer (in preparation).

The transfer of Chernobyl caesium in the surveyed water bodies can be described as a chain of five stations (Fig. 1): (1) fallout, represented by the regional ^{137}Cs value of grass [33]; (2) sediment, with the riparian soil as a side branch; (3) the acid(HNO_3)-extractable fraction of the sediment; (4) the salt-exchangeable fraction ("solution"); and (5) the plant. The first evaluation had divided the transfer into the retention of fallout by the sediment and the transfer to the plant

[28], a later summary into retention, sorption–desorption, uptake and translocation [32], and the chain fallout → sediment → soil solution → plant was drawn as a sketch in a later book [34, pp. 29, 33], but the solution step was not quantified. The present paper deals with stations 2, 4 and 5. Each sediment had been shaken with a dilute salt solution, and the desorbed activity was counted. The solution factor LF (German *Lösungsfaktor*) = $C_{solution}$ / $C_{sediment}$ and the nutrition factor NF (German *Nahrungsfaktor*) = C_{plant} / $C_{solution}$, where C denotes the activity concentration at each station, split the transfer factor into a physico-chemical and a biological step, TF = LF × NF. On logarithmic scales the two steps add up to the total transfer, and so do their slopes against any explanatory variable. This three-station model (stations 2 → 4 → 5) can therefore locate where a dependence of TF arises. Station 3, the acid extract, lies between sediment and solution; it was measured routinely only for stable potassium and caesium, and its use for the ladder of binding strengths of potassium is presented separately on the same desorption data (Ahamer, in preparation). Station 1 and the retention of fallout by the sediment are treated in Ahamer (in preparation). The present paper is restricted to the caesium results of the three-station model and to the potassium values needed to compare the two elements.

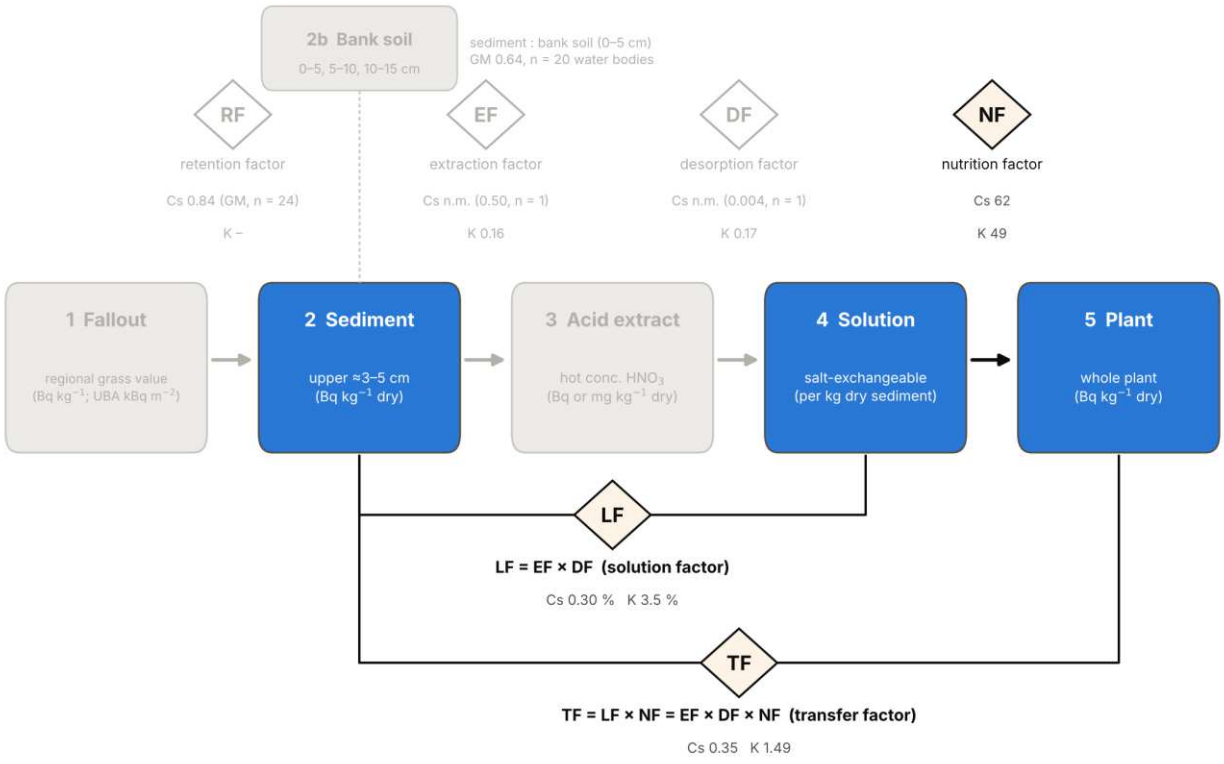


Fig. 1 The five-station chain of caesium and potassium transfer in the surveyed water bodies (1 fallout, 2 sediment with the riparian soil as side branch 2b, 3 acid extract, 4 salt-exchangeable solution, 5 plant) with the transfer factors between the stations: RF, retention factor (sediment / regional grass value); EF, extraction factor (acid extract / sediment); DF, desorption factor (solution / acid extract); NF, nutrition factor (plant / solution); LF = EF × DF, solution factor (solution / sediment); TF = LF × NF, transfer factor (plant / sediment). Rectangles denote activity concentrations at the stations, rhombi the quotients (factors) between them, following the presentation convention of

Ahamer [34]. This paper treats the three-station model sediment → solution → plant (stations 2, 4 and 5, coloured); the acid-extract station 3 and the other parts (grey) are treated in companion papers. All factors are ratios of dry-mass concentrations (Bq kg^{-1} or mg kg^{-1}); RF uses the regional grass contamination map [33] as fallout proxy. Values: medians of LF and NF per site-season, geometric means of TF per plant sample and of RF per water body (n.m., not measured: single pilot extract of one pond); ^{137}Cs decay-corrected to 26 April 1986. On logarithmic scales the steps add up to the total transfer, and so do their slopes against sediment activity. LF, solution factor (activity desorbed into the salt solution per kg dry sediment / activity in the sediment); NF, nutrition factor (activity in the plant / activity in the solution); TF, transfer factor (activity in the plant / activity in the sediment); all on a dry-weight basis, caesium decay-corrected to 26 April 1986

We ask: (1) How are LF, NF and TF distributed? (2) Do caesium and potassium differ in the solution step, in the uptake step or in both? (3) Which step carries the decline of TF with contamination, and how robust is the answer to ratio coupling, sampling error and the detection limits of the solutions? (4) Which alternative mechanisms could produce a declining LF, and which of them can the data test? (5) How do the sediment activities relate to ^{137}Cs in the riparian soils?

2. Material and methods

2.1 Survey and gamma spectrometry

Sites, sampling and measurements are documented in the data paper (Ahamer, in preparation) and in the transfer-factor re-examination (Ahamer, submitted to J. Environ. Radioact.); only the points needed here are summarised. The 26 water bodies (ponds, lakes, oxbows, fens and bog-meadow streams, 350–1750 m above sea level) were sampled in August–September and in November 1987. Throughout this paper, a site-season denotes one water body in one sampling campaign (summer or autumn 1987); it is the unit at which sediment, solution and plants were measured together. The upper ≈3–5 cm of sediment was taken with a mud grab as a single sample per site-season; plants were sampled above ground and rinsed. All samples were counted fresh in 1-L Marinelli beakers on a Ge(Li) detector at the Reactor Institute Graz. Every activity and ratio in this paper refers to dry weight (Bq kg^{-1} dry weight), because the adhering water of aquatic plants cannot be standardised. Caesium activities of all compartments were decay-corrected to 26 April 1986, so that ratios between compartments share one reference date. The median relative counting error (1σ) of ^{137}Cs was 2.0% for the sediments and 3.2% for the plants. Values entered with a nominal error of 100% are invalid manual entries and were not used. Sediment properties (loss on ignition, pH, particle-size distribution and the relative mineral contents of the clay fraction) are described in the companion papers.

2.2 Desorption experiment

In autumn 1988, about 30 g of each sediment were shaken intensively for about 24 h with a dilute salt solution, most probably $CaCl_2$ according to the laboratory notes of the time. If the reagent was $CaCl_2$, LF mainly indexes the caesium on regular exchange sites, and the ^{40}K in solution stems from the sediment (see the companion paper on uncertainties, Ahamer, in preparation). The 30 g most probably refer to the total (wet) mass of the sediment. The concentration and volume of the reagent, the separation of solution and solid, the reagent blank and the storage of the sediments since sampling are not documented. The solutions were counted with long counting times between 1 and 19 October 1988 (889–907 days after the accident, 11–14 months after sampling); the counted solution masses were 20–200 g (median 123 g; n = 40). The desorbed activity was expressed per kilogram of dry sediment and decay-corrected to 26 April 1986.

The counting errors of the solutions were never recorded (the database has a variable for them, which was left empty), although the 1991 report noted a considerable statistical error despite long counting times [30, p. 93]. We therefore estimated them from the relation between relative counting error and counted ^{137}Cs activity in 281 measurements on the same detector, $\log_{10} \sigma_{rel}(\%) = 1.043 - 0.360 \log_{10} a$ ($r = -0.81$), where a is the counted ^{137}Cs activity in the beaker in Bq. For 30 g of dry sediment per test, the solutions contained a median of 0.095 Bq ^{137}Cs (0.002–1.3 Bq), with an estimated median counting error of 26%, and for 10 of 34 solutions the estimated error exceeded 30%; such values lie close to the detection limit [35, 36]. For the more probable 30 g of wet sediment, the activities were about 3.5 times lower (median 0.027 Bq; median estimated error 41%), and 28 of 34 solutions exceeded 30%. The single water sample, counted on the same detector at 0.18 Bq with 44% error against a model value of 21%, suggests that the model rather underestimates the errors.

The solution and nutrition factors are

$$LF = C_{solution} / C_{sediment} \text{ and } NF = C_{plant} / C_{solution},$$

where $C_{sediment}$ and C_{plant} are activity concentrations in Bq kg^{-1} dry weight and $C_{solution}$ is the activity found in the solution divided by the dry mass of the sediment shaken, in Bq desorbed per kg dry sediment; hence $TF = C_{plant} / C_{sediment} = LF \times NF$. The same symbols are used for ^{137}Cs, ^{134}Cs and ^{40}K; where needed, the nuclide is given as an index (e.g. LF_{137}, LF_{134}, LF_K). NF is not a concentration factor relative to water: its unit is (Bq kg^{-1} plant)/(Bq desorbed per kg sediment), and it measures enrichment relative to the desorbable pool of the sediment, not relative to a pore-water concentration. In the original files the plant activity entering NF referred

to the counting date and the solution activity to the accident date, which made the stored NF about 3.5% too low; all factors were recomputed here on the common reference date. ^{40}K activities were converted to potassium mass with 32.32 mg K kg^{-1} per Bq kg^{-1}.

2.3 Data selection

^{137}Cs in solution was measured for 37 site-seasons. Two of them lacked a sediment sample of their own. One solution (pa, summer; 213 Bq kg^{-1} ^{137}Cs against 11.3 Bq kg^{-1} ^{134}Cs) is probably a decimal error (Section 3.1) and was excluded, so that LF of ^{137}Cs was available for 34 site-seasons at 23 water bodies. LF of ^{40}K was available for 25 site-seasons; the ^{40}K value of the pu summer sediment (counting error 99%, marked as an uncertain manual evaluation) is invalid. LF of ^{134}Cs, owing to its decay, was available for only 4 site-seasons (NF for 3); seven plant samples with an invalid ^{134}Cs value (99.9% error code) were excluded from all ^{134}Cs analyses, leaving 133. Of the 144 whole-plant samples, four with 74–94% dry matter, probably dead plant material, were excluded from the transfer analyses; water drained from plant samples is not plant tissue. This left 140 plant samples, of which 120 had a sediment of their own for TF and 110 a solution value for NF. All three exclusions were reversed in sensitivity analyses (Section 3.5; Table S1).

2.4 Statistical units and estimators

LF exists once per sediment sample, so the site-season is the unit of analysis. For each site-season, NF is the median activity of its plant samples divided by the solution activity, and TF the same median divided by the sediment activity, so that log TF = log LF + log NF holds exactly (34 site-seasons with NF, 32 with all three factors). Plant samples are used only descriptively, because samples of one site-season share a single solution value. Logarithms are to base 10; geometric means (GM) and geometric standard deviations (GSD) summarise the log-normal distributions [37]. We give Pearson's r of the logarithms together with Spearman's rank coefficient ρ [38], which is robust against outliers and does not depend on the transformation.

Slopes against log sediment ^{137}Cs were estimated by ordinary least squares with t-based 95% confidence intervals (CI). Robustness was assessed by a cluster bootstrap that resamples whole water bodies (2000 replicates) [39], by mixed models with the water body as random intercept, by the Theil–Sen estimator [40], by site means and by influence analyses that removed the least or most contaminated site-seasons one at a time. Because the slopes of log LF and log NF add up to that of log TF, the share of the TF slope carried by LF was estimated with its bootstrap CI. Effects of censoring were examined in three ways: by excluding solutions with an estimated counting error above 30%, by weighted least squares with weights $1/(\sigma_{count}^2 + 0.2^2)$ in log units,

and by a Tobit (censored) regression [41, 42]. In the Tobit model, values with an estimated error above 30% (and, as sensitivity, above 40% or 50%) enter as upper limits, because results reported near a decision threshold are selected towards high values.

Ratios that share a denominator are coupled [43–45]. A permutation null model, in which solution activities were shuffled among sediments, gives the LF slope expected if the solution were unrelated to the sediment; the same shuffle gives the null distribution of the correlation between log LF and log NF. The representativeness error of a single grab sample σ_u was taken from the summer–autumn differences of sediment ^{137}Cs at 18 water bodies, $\sigma_u = SD(\Delta\log)/\sqrt{2} = 0.32$ (χ^2 95% CI 0.24–0.47; robust estimate 0.41; Ahamer, in preparation). Both values are upper bounds, because they include real seasonal change. Slopes were corrected by regression calibration with the reliability ratio $\kappa = 1 - \sigma_u^2/\mathrm{var}(\log C_{sediment})$ [46, 47]. The uncertainty of σ_u was propagated by drawing it from its scaled χ^2 distribution within the cluster bootstrap; SIMEX served as a check [48]. How this error affects LF depends on what LF responds to. If the desorbable fraction is a property of the counted sediment itself (assumption A), LF is unaffected, because the solution was prepared from that sediment. If it responds to the contamination of the site as a whole (assumption B), its slope is attenuated like that of TF. Both cases are reported. Heterogeneity between the 30 g aliquot and the counted beaker adds noise to LF; its effect was simulated for $\sigma = 0.1$ and 0.2 log units.

The same three-panel decomposition (TF, LF and NF against the sediment value) was applied to ^{40}K, to ^{134}Cs and to two quotients of nuclides. ^{134}Cs (half-life 2.06 years) in the 1987 samples stemmed from Chernobyl alone, whereas ^{137}Cs also contained caesium from the nuclear-weapons tests. With the ^{137}Cs/^{134}Cs activity ratio of Chernobyl deposition, 1.90 on 26 April 1986 [49], a value also given as about 1.90 by Ahamer et al. [29], the weapons-test share of the ^{137}Cs in a sample with the decay-corrected ratio R is $1 - 1.90/R$. As a sensitivity analysis we used the release ratio of the accident, 1.82 on 26 April 1986 [50]. If weapons-test caesium, deposited decades earlier, were less desorbable or less available to plants than Chernobyl caesium, LF_{137}/LF_{134} and TF_{137}/TF_{134} would lie below one, whereas NF_{137}/NF_{134} should equal one, because a plant cannot discriminate between two isotopes in the same solution. If weapons-test caesium were completely unavailable, the plant ratio would be constant at 1.90, and $TF_{137}/TF_{134} = 1.90/R$ would decline against R with a slope of exactly –1; if both sources were equally available, the plant ratio would follow the sediment ratio, and the slope corrected for counting errors would be 0. We therefore plotted the three isotope quotients against the sediment ratio R. We preferred R to the derived weapons-test share because it is the measured quantity and because counting errors place R below 1.90, and the share below zero, for 7 of 42 sediments

(3 below 1.82). The relative availability was also estimated directly as $TF_{bomb}/TF_{Chernobyl}$ = [f_p/(1 – f_p)]/[f_s/(1 – f_s)], where f_s and f_p are the weapons-test shares computed from the geometric mean ratios of the sediments and of the plants, with a cluster-bootstrap CI. To examine the competition of potassium, LF_{Cs}/LF_K, NF_{Cs}/NF_K and TF_{Cs}/TF_K (^{137}Cs over ^{40}K) were plotted against the sediment $^{137}Cs/^{40}K$ activity ratio, which measures the supply of caesium relative to its competitor. For quotients whose denominator contains the abscissa (TF, LF and their ratios), the slope has a natural scale. A slope of 0 means that the numerator is proportional to the abscissa, and a slope of –1 that it is independent of it; –1 is also the mean of a permutation null model in which the numerator was shuffled among site-seasons (for NF panels the null value differs from 0 and was taken from the permutations). For the isotope quotient, the null value of –1 coincides with the prediction of complete unavailability of weapons-test caesium. Counting errors of the abscissa enter such quotients with the opposite sign. We therefore corrected these slopes with the reliability ratio κ computed from the stored counting errors of the sediment values, b = (slope + 1 – κ)/κ (for NF, b = slope/κ). Geometric means of the quotients were compared with one by t-tests on the logarithms, with cluster-bootstrap CIs. The decompositions of Section 3.4 are exploratory. Their p values were adjusted for multiplicity by the Benjamini–Hochberg procedure over all 27 tests of that section with at least 10 site-seasons (q values in Table S3), and only results with $q < 0.05$ that are not explained by ratio coupling are interpreted. Panels with four or fewer site-seasons are shown for illustration only and were not tested.

Confounding by organic matter, dry matter and grain size was tested with joint regressions of log LF on log $C_{sediment}$ and each covariate, with variance inflation factors (VIF). Mineral contents, particle-size fractions, altitude, catchment area and catchment geology were determined once per water body (the mineral and grain-size values had been copied into both season rows of the original file); they were therefore analysed at the water-body level (mean log LF and mean log $C_{sediment}$ of the site-seasons of a water body), whereas loss on ignition, dry matter, pH and sediment ^{40}K, measured in every sample, were analysed per site-season. Seventeen sediment and catchment descriptors were screened against LF, both directly and after removing the dependence on sediment ^{137}Cs (34 tests), with false-discovery-rate control [51]. The geology of the catchments was coded from the site table of 1987 with the Geological Map of Styria (Ahamer, in preparation) [52]. Equality of NF for caesium and potassium was examined at the site-season level by two one-sided tests (TOST) [53] with equivalence margins of a factor of 1.5 and 2. Sediment ^{137}Cs was compared with ^{137}Cs in the 0–5 cm layer of the riparian soil at the site level (season duplicates removed). The relation between the sediment-to-

soil ratio and LF, which share $C_{sediment}$, was tested against a permutation of the soil values. Analyses used Python 3 with SciPy and statsmodels [54].

3. Results

3.1 Distributions of LF, NF and TF

All three factors were approximately log-normally distributed (Fig. 2; Table 1). LF of ^{137}Cs had a median of 0.30% and a GM of 0.35% (95% CI 0.25–0.52%; GSD 2.9; n = 34), ranging from 0.05% (hs, summer) to 6.5% (ri, summer). The excluded pa summer solution would have given 10.9%, 36 times the median. Its ^{137}Cs/^{134}Cs ratio (18.8) was ten times that of its sediment (1.8). Read as 21.3 instead of 213 Bq kg^{-1}, the solution would have the isotope ratio of 1.9, close to that of its sediment and of Chernobyl caesium, and an LF of 1.1%, so that a decimal error is the most probable explanation. At the four other site-seasons with both isotopes, LF of ^{134}Cs and ^{137}Cs agreed within a factor of 0.83–1.45 (GM 1.07). LF of ^{40}K had a median of 3.5% (GM 2.8%; n = 25). NF of ^{137}Cs had a median of 62 (GM 72, 95% CI 47–109; n = 34), and NF of ^{40}K a median of 49 (GM 63; n = 23). Per plant sample, the median NF of ^{137}Cs was 80 (n = 110); this higher descriptive value reflects the different unit, not a different estimate. TF of ^{137}Cs had a GM of 0.35 (n = 120), and TF of ^{40}K a GM of 1.49 (n = 96), with a much narrower distribution (GSD 2.1 against 3.7). The 1991 evaluation had reported 0.31% for the median LF and 49 for the median NF of ^{137}Cs [30, Section 6.5]; the difference in NF stems from the common reference date and the exclusions of Section 2.3.

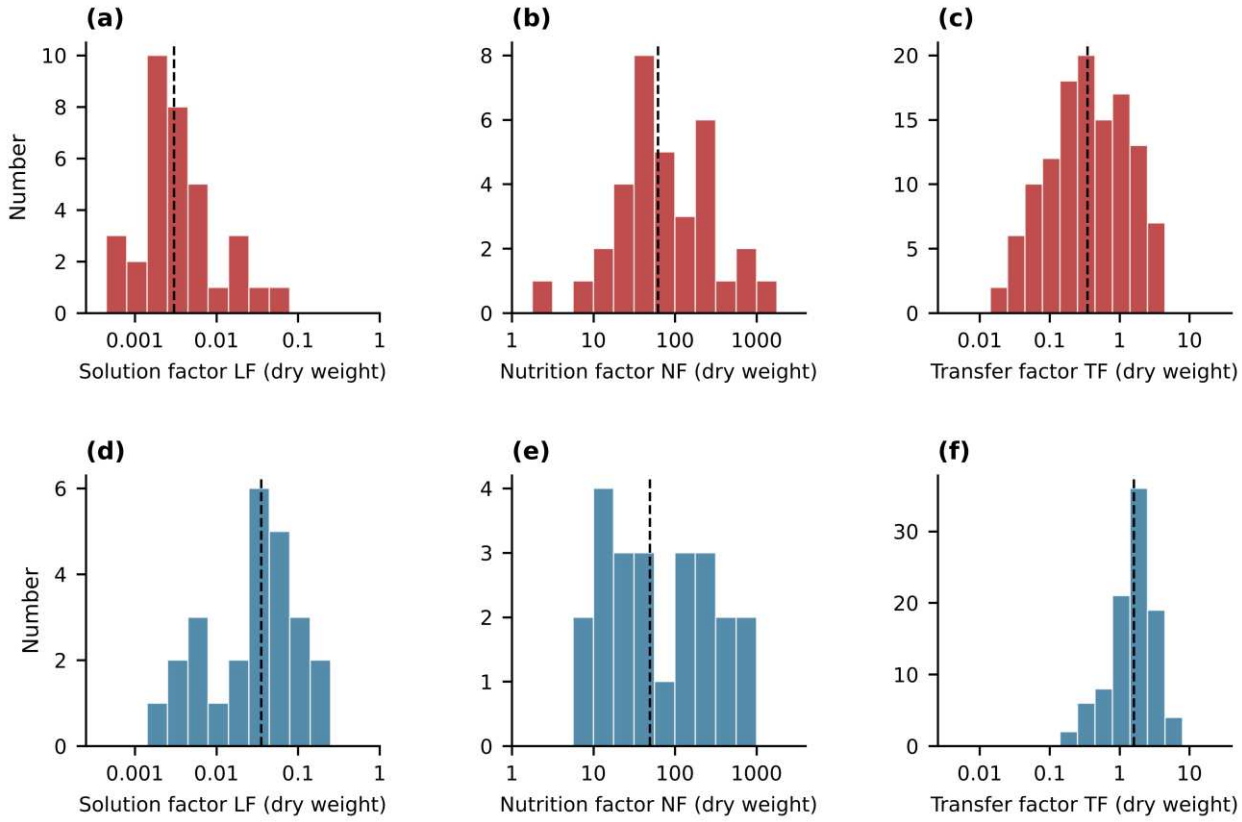


Fig. 2 Frequency distributions of the solution factor LF, the nutrition factor NF and the transfer factor TF of ^{137}Cs (top, red) and ^{40}K (bottom, blue) on logarithmic axes; dashed lines are medians; GSD, geometric standard deviation. (a) LF ^{137}Cs, site-seasons: n = 34, median 0.30%, GSD 2.9; (b) NF ^{137}Cs, site-seasons: n = 34, median 62.3, GSD 3.8; (c) TF ^{137}Cs, plant samples: n = 120, median 0.348, GSD 3.7; (d) LF ^{40}K, site-seasons: n = 25, median 3.5%, GSD 3.6; (e) NF ^{40}K, site-seasons: n = 23, median 49.3, GSD 4.2; (f) TF ^{40}K, plant samples: n = 96, median 1.61, GSD 2.1. LF and NF are given per site-season (NF = median plant activity / solution activity), TF per plant sample with a sediment of its own. Abbreviations as in Fig. 1

Table 1 Distributions of the solution factor LF, the nutrition factor NF and the transfer factor TF (dry weight; caesium decay-corrected to 26 April 1986). GM, geometric mean; GSD, geometric standard deviation; P5–P95, 5th to 95th percentile. Site-season NF and TF use the median plant activity of the site-season; values per plant sample are descriptive (samples of one site-season share the solution value). Abbreviations as in Fig. 1

Factor	Nuclide	Unit	n	Median	GM	GSD	P5–P95	Range
LF	^{137}Cs	site-season	34	0.3%	0.35%	2.9	0.072%–2.2%	0.055%–6.5%
LF	^{134}Cs	site-season	4	0.34%	0.48%	3.2	0.2%–2.2%	0.19%–2.6%
LF	^{40}K	site-season	25	3.5%	2.8%	3.6	0.38%–15%	0.18%–23%
NF	^{137}Cs	site-season	34	62.3	72.4	3.8	10.2–671	3.14–1 059
NF	^{40}K	site-season	23	49.3	63	4.2	8.22–569	6.66–583
NF	^{137}Cs	plant sample (descriptive)	110	80.5	79.5	4.7	5.17–812	1.57–1 932
TF	^{137}Cs	site-season	32	0.348	0.275	3.5	0.0311–1.69	0.0244–2.94
TF	^{137}Cs	plant sample	120	0.348	0.347	3.7	0.0341–2.55	0.0147–4.41
TF	^{40}K	plant sample	96	1.61	1.49	2.1	0.346–4	0.153–7.66

The median potassium content was about 16 800 mg kg^{-1} in the sediments (n = 37), 560 mg per kg of sediment in the solution (n = 29) and 28 600 mg kg^{-1} in the plants (n = 139). At the 11

water bodies with LF in both seasons, LF of ^{137}Cs in autumn was 0.90 times that in summer (paired t-test p = 0.72), and the two seasons were weakly correlated (ρ = 0.39).

3.2 Potassium leaves, caesium stays

At the 20 site-seasons (16 water bodies) with both values, LF of ^{40}K exceeded LF of ^{137}Cs by a factor of 8.1 (GM; 95% CI 4.4–14.8; median 9.0; also listed in the data paper, Ahamer, in preparation). Potassium was released more readily at 18 of the 20 site-seasons (Wilcoxon p < 0.001; Fig. 3a), and the two LF were only weakly correlated (r = 0.32, ρ = 0.25). In the uptake step, NF of ^{137}Cs was 1.04 times NF of ^{40}K (GM over 23 site-seasons; 95% CI 0.48–1.83; Wilcoxon p = 0.46; r = 0.34; Fig. 3b). The 90% CI (0.58–1.85) lies within an equivalence margin of a factor of two (TOST p = 0.032) but not within a factor of 1.5 (p = 0.14).

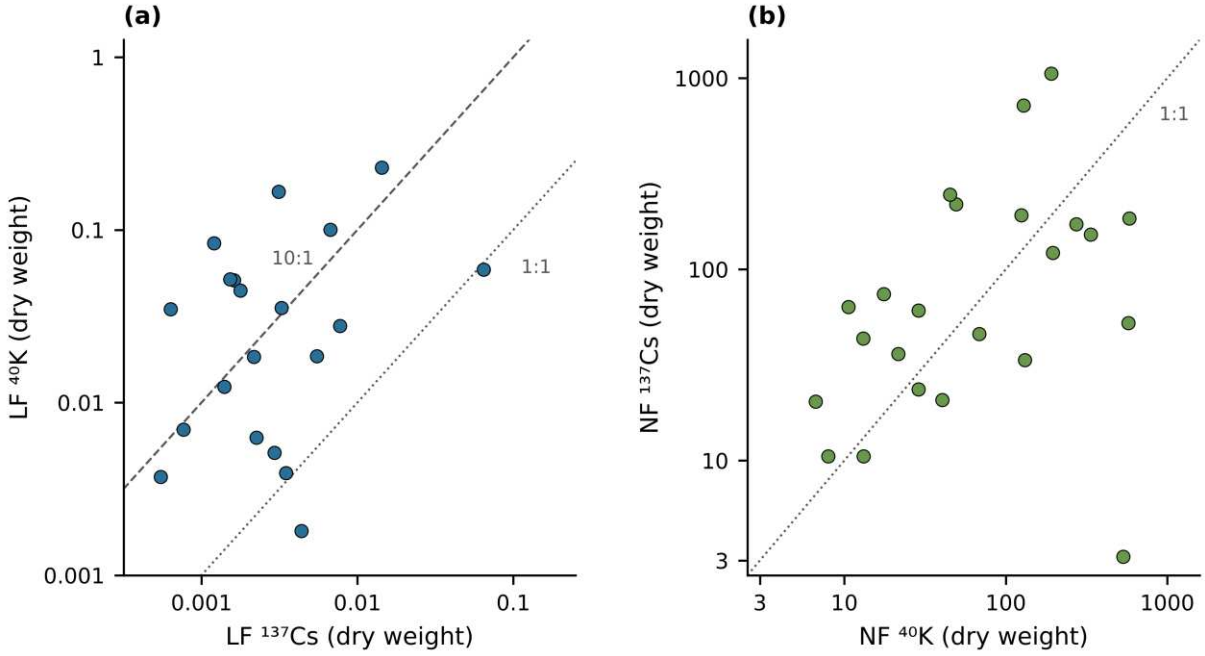


Fig. 3 Potassium leaves, caesium stays. (a) Solution factor LF of ^{40}K against that of ^{137}Cs at the site-seasons with both values (dotted 1:1, dashed 10:1). (b) Nutrition factor NF of ^{137}Cs against that of ^{40}K per site-season (median plant activity / solution activity; dotted 1:1). Geometric mean ratios: (a) LF_K/LF_{Cs} = 8.1 (95% CI 4.4–14.8; n = 20 site-seasons); (b) NF_{Cs}/NF_K = 1.04 (95% CI 0.48–1.83; n = 23 site-seasons); confidence intervals by cluster bootstrap over water bodies. Potassium is released several times more readily from the sediment; between solution and plant no difference between the elements is detectable. Abbreviations as in Fig. 1

Because $TF_{Cs}/TF_K = (LF_{Cs}/LF_K) \times (NF_{Cs}/NF_K)$ holds exactly, the contrast between the elements can be located. At the 19 site-seasons with all four values, the ratio of the transfer factors was 0.17. It was the product of an LF ratio of 0.12 (95% CI 0.07–0.23; Wilcoxon p < 0.001) and an NF ratio of 1.33 (95% CI 0.83–2.34; p = 0.29). The solution step accounted for 116% of the logarithmic contrast (95% CI 90–158%). Accordingly, the median ^{137}Cs/^{40}K activity ratio fell from 2.7 in the sediments to 0.41 in the solutions and changed little to 0.30 in the plants. In the plant samples, TF of ^{40}K was on average 3.8 times that of ^{137}Cs (n = 96).

3.3 Decomposition of the decline of TF

Across all 34 site-seasons, log LF declined with log sediment ^{137}Cs with a slope of –0.36 (95% CI –0.58 to –0.14; p = 0.003; r = –0.50, ρ = –0.45; bootstrap –0.63 to –0.08): the desorbed activity rose as the 0.64th power of the sediment activity. At the 32 site-seasons (23 water bodies) with all three factors, log TF declined with a slope of –0.55 (–0.78 to –0.33), log LF with –0.39 (–0.61 to –0.17; p < 0.001) and log NF with –0.16 (–0.45 to +0.13; p = 0.26) (Fig. 4; Table 2). The slopes add up exactly. The share of the TF slope carried by LF was 70%, with a bootstrap 95% CI of 19% to 129%. For orientation, the TF slope over all 39 site-seasons with plants and their own sediment was –0.51.

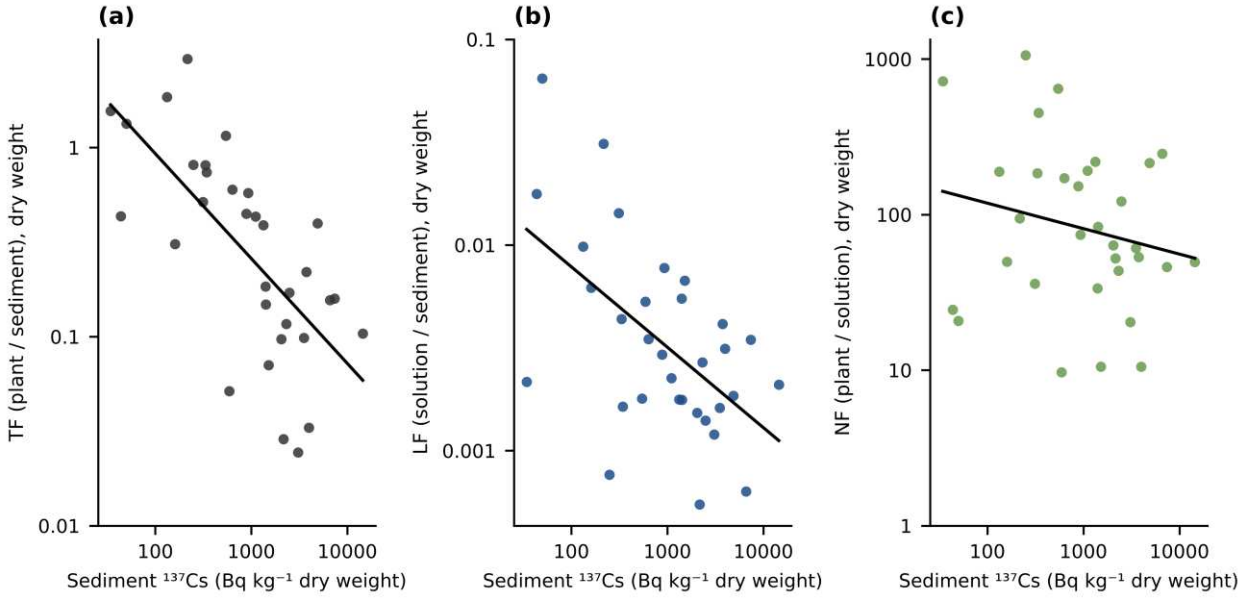


Fig. 4 Decomposition of the transfer factor at the site-season level (n = 32): (a) TF of ^{137}Cs (median plant activity / sediment activity), (b) solution factor LF, (c) nutrition factor NF = TF/LF, each against the sediment ^{137}Cs activity, with least-squares lines (slopes and alternative estimators in Table 2). Because log TF = log LF + log NF, the slopes add up. Abbreviations as in Fig. 1

Table 2 Slopes of log TF, log LF and log NF of ^{137}Cs against log sediment ^{137}Cs at the site-season level, with alternative estimators and sensitivity analyses. The slopes of LF and NF add up to that of TF for every linear estimator fitted to the same data. Censoring analyses assume 30 g of dry sediment per test. σu, representativeness error of single grab samples (upper bound); κ, reliability ratio; assumption A, LF depends on the counted sediment itself (not affected by σu); assumption B, LF depends on site-level contamination. Abbreviations as in Fig. 1

Estimate	log TF	log LF	log NF
OLS slope (95% CI), n = 32	–0.55 (–0.78 to –0.33)	–0.39 (–0.61 to –0.17)	–0.16 (–0.45 to +0.13)
p (OLS); Pearson r / Spearman ρ	< 0.001; –0.68 / –0.73	< 0.001; –0.56 / –0.50	0.259; –0.21 / –0.20
Cluster bootstrap 95% interval	–0.89 to –0.37	–0.66 to –0.12	–0.54 to +0.11
Mixed model, water body random intercept (95% CI)	–0.65 (–0.86 to –0.44)	–0.39 (–0.60 to –0.18)	–0.21 (–0.53 to +0.11)
Theil–Sen slope	–0.55	–0.42	–0.21
Site means (n = 23)	–0.63 (p < 0.001)	–0.42 (p 0.006)	–0.21 (p 0.253)
With pa summer as stored (n = 33)	–0.54 (p < 0.001)	–0.35 (p 0.011)	–0.19 (p 0.212)

Share of TF slope in LF (bootstrap 95% CI)		70% (19–129%)	
LF, all 34 site-seasons (95% CI)		–0.36 (–0.58 to –0.14); p 0.003	
LF without the 3 least contaminated (n = 31)		–0.31 (p 0.024)	
LF, solutions with est. error ≤ 30% only		–0.65 (p < 0.001, n = 24)	
LF, error-weighted least squares		–0.44	
LF, Tobit, 10 values > 30% as upper limits		–0.15	
Sampling error corrected, σu = 0.32 (κ = 0.77), assumption A	–0.43	–0.39 (unchanged)	–0.03
Same, assumption B (LF attenuated like TF)	–0.43	–0.50	+0.08
Regression calibration with uncertain σu, A (95% CI)	–0.41 (–0.79 to +0.07)	(unchanged)	–0.00 (–0.47 to +0.52)
Same, assumption B (95% CI)	–0.41	–0.54 (–1.27 to –0.15)	+0.13 (–0.38 to +1.20)

The alternative estimators agreed in sign and order of magnitude (Table 2). For LF (34 site-seasons), the mixed model gave –0.35 (95% CI –0.59 to –0.12), Theil–Sen –0.38 and site means –0.40 (p = 0.009, n = 23). For NF they gave –0.21 (–0.53 to +0.11), –0.21 and –0.21 (p = 0.25).

3.4 Potassium, caesium-134 and the two quotients

Potassium-40. At the 20 site-seasons (16 water bodies) with all three factors of ^{40}K, the sediment ^{40}K varied only fivefold (221–1101 Bq kg^{-1}; Fig. 5). TF of ^{40}K declined with sediment ^{40}K with a slope of –0.53 (95% CI –1.20 to +0.15; p = 0.12), between proportional transfer (0) and a plant potassium independent of the sediment (–1). LF of ^{40}K declined steeply (–2.06; –3.39 to –0.72; p = 0.005, q = 0.016), but within the range expected from ratio coupling alone (permutation null –1.00, 95% range –2.26 to +0.28; p = 0.12); solution potassium was not significantly related to sediment potassium (slope –1.06, r = –0.36, p = 0.11). NF of ^{40}K rose (+1.53; –0.03 to +3.09; p = 0.054, q = 0.10), also within the range of its permutation null (+1.05; 0.42 to 1.71). None of the three slopes differed from its permutation null value (–1 for TF and LF, +1.05 for NF) by more than the permutation range (p ≥ 0.12); corrected for the counting error of sediment ^{40}K (κ = 0.90), they were –0.47, –2.18 and +1.71. At these 20 site-seasons, plant potassium was not significantly related to sediment potassium (r = +0.33, p = 0.16; ρ = +0.23) or to solution potassium (ρ = –0.08). Over the 23 complete potassium chains of the companion paper on the potassium ladder, plant potassium rose with total sediment potassium (r = 0.45, p = 0.03), but not significantly at the water-body level (p = 0.10; Ahamer, in preparation). Tentatively, LF of ^{40}K was higher in organic sediments (ρ = +0.47 with loss on

ignition, p = 0.044, q = 0.085, n = 19), which contained less total potassium (ρ = –0.51, p = 0.024, q = 0.055).

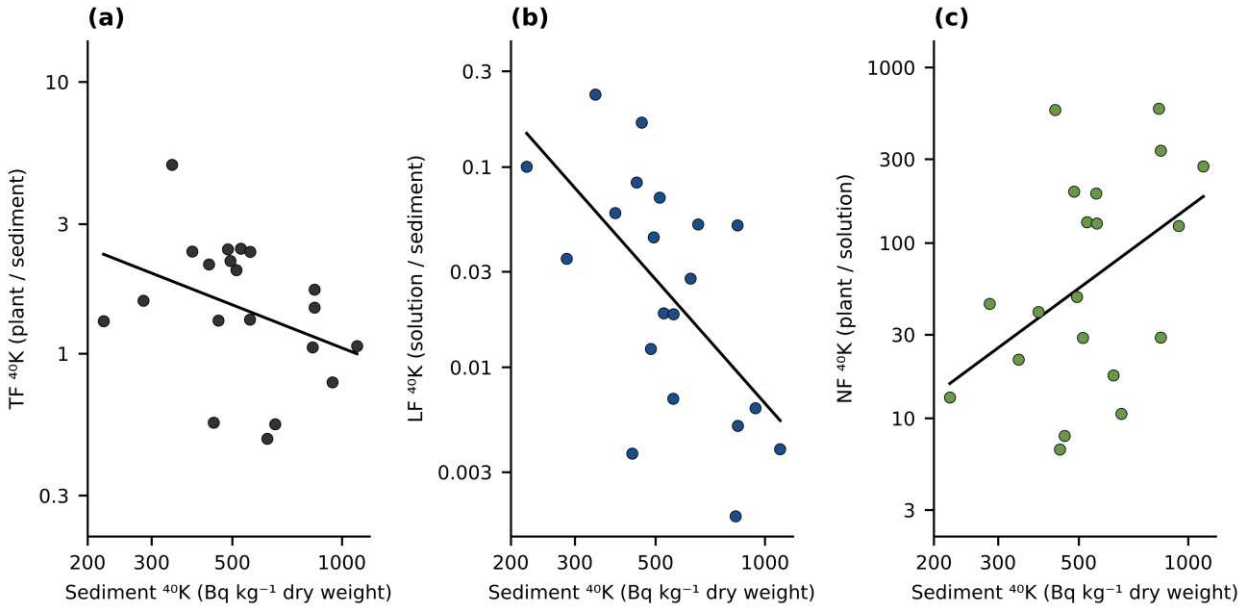


Fig. 5 Decomposition of the transfer of ^{40}K at the site-season level: (a) TF of ^{40}K (median plant activity / sediment activity), (b) LF of ^{40}K (solution / sediment), (c) NF of ^{40}K (plant / solution), each against the sediment ^{40}K activity, with least-squares lines; n = 20 site-seasons at 16 water bodies. Slopes, permutation null values (TF and LF –1, NF +1.05), corrected slopes and q values in Table S3; no slope differs from its null value. Abbreviations as in Fig. 1

Caesium-134. TF of ^{134}Cs declined with sediment ^{134}Cs with a slope of –0.66 (95% CI –0.88 to –0.45; p < 0.001; r = –0.73; 38 site-seasons, 23 water bodies; Fig. 6a). This is clearly less steep than the null value of –1 (permutation range –1.23 to –0.77; p = 0.003, q = 0.011) and similar to the slope of TF of ^{137}Cs at the same site-seasons (–0.61). The counting errors of sediment ^{134}Cs (median 4.3%) do not affect this slope (κ = 1.00); corrected also for the grab-sample error (σ_u = 0.32), the slope would be about –0.57, still clearly above –1. LF and NF of ^{134}Cs exist for only 4 and 3 site-seasons (Fig. 6b, c); these panels are illustrative only and were not tested. At these site-seasons LF of ^{134}Cs was 0.83–1.45 times that of ^{137}Cs. The ^{134}Cs value of the pa summer solution, whose ^{137}Cs value is suspect, would give an LF of 1.0%.

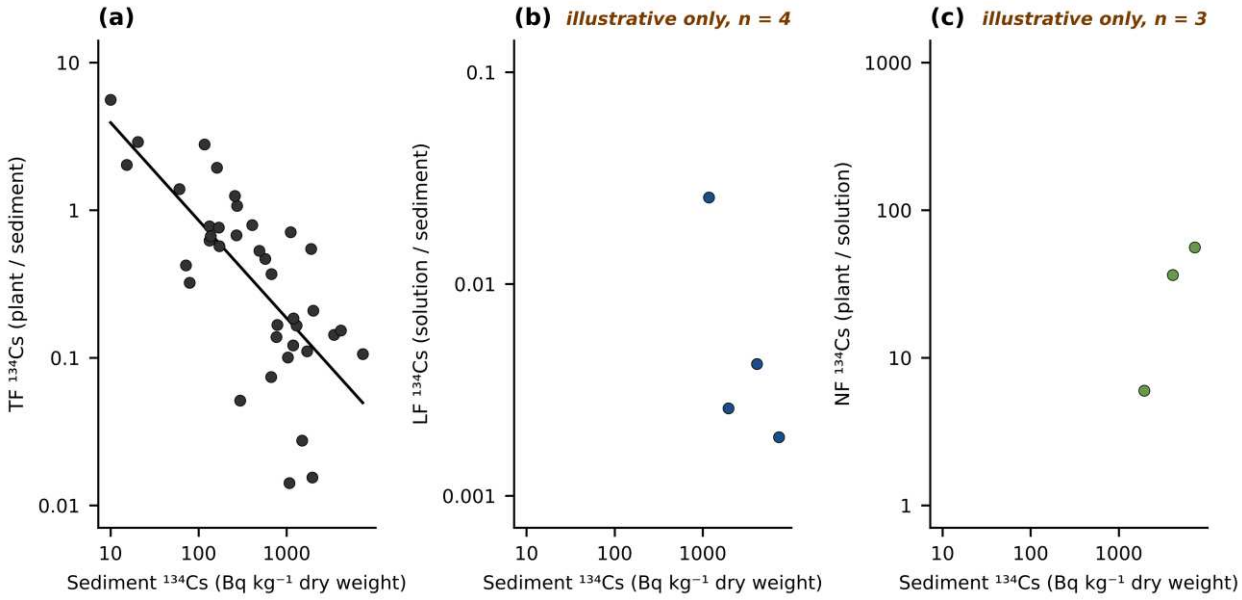


Fig. 6 Decomposition of the transfer of ^{134}Cs, which stems from the Chernobyl fallout alone: (a) TF of ^{134}Cs (median plant activity / sediment activity), (b) LF of ^{134}Cs (solution / sediment), (c) NF of ^{134}Cs (plant / solution), each against the sediment ^{134}Cs activity (decay-corrected to 26 April 1986). (a) n = 38 site-seasons at 23 water bodies, least-squares line; statistics in Table S3. (b) and (c) illustrative only, n = 4 and 3: ^{134}Cs in solution was reported for only four site-seasons; no line fitted, no inference. Plant samples with an invalid ^{134}Cs value (99.9% error code) excluded. Abbreviations as in Fig. 1

Isotope ratio. The decay-corrected ^{137}Cs/^{134}Cs ratio of the sediments had a median of 2.02 (1.77–2.89; n = 42), corresponding to a median weapons-test share of 6% of the sediment ^{137}Cs (–7% to 34%). The plants had a median ratio of 1.98 (1.75–4.32; 38 site-seasons). On average, TF of ^{137}Cs equalled TF of ^{134}Cs (TF_{137}/TF_{134}: GM 1.00, 95% CI 0.92–1.11; p = 0.99; Fig. 7a). If the weapons-test caesium had not been transferred at all, the expected value would have been 0.92, at the lower limit of this interval; the geometric mean ratio of the plants (2.07) exceeded 1.90 (p = 0.007, q = 0.02), so the plants did contain weapons-test caesium. TF_{137}/TF_{134} declined with the sediment ratio (slope –1.10; 95% CI –1.67 to –0.52; p < 0.001), and this slope equals the null value of –1.00 (permutation range –1.46 to –0.37; p = 0.73): the isotope ratio of the plants did not follow that of their sediment (ρ = +0.07). Note that a slope of –1 is also what a complete unavailability of weapons-test caesium predicts (plant ratio constant at 1.90), whereas equal availability predicts a corrected slope of 0. The counting errors of ^{137}Cs and ^{134}Cs account for about half of the variance of log R (κ = 0.52); the corrected slope was –1.19 (–2.29 to –0.09). It excludes equal availability, while the mean ratio (1.00) favours it. Expressed directly, the transfer of weapons-test relative to Chernobyl caesium was 0.99 (cluster-bootstrap 95% CI 0.28–2.67). With the release ratio of 1.82 [50] instead of 1.90, the median weapons-test share rose to 10% (–3% to 37%; 3 sediments below 1.82), the value expected for complete unavailability fell to 0.88, outside the CI of the mean ratio, and the relative transfer was 0.99

(0.48–1.98); the slopes do not depend on this constant. LF_{137}/LF_{134} (GM 0.93; n = 4) and NF_{137}/NF_{134} (GM 1.27; n = 3) are illustrative only (Fig. 7b, c).

Caesium relative to potassium. At the 19 site-seasons with all four factors, the sediment $^{137}Cs/^{40}K$ ratio was governed by ^{137}Cs ($\rho = 0.96$ with sediment ^{137}Cs). TF_{Cs}/TF_K declined with this ratio with a slope of –0.64 (95% CI –0.93 to –0.35; $p < 0.001$; $r = –0.75$), less steeply than the null value of –1.00 (permutation range –1.31 to –0.70; $p = 0.017$, $q = 0.04$; Fig. 7d). The decline arose in the solution step: LF_{Cs}/LF_K declined with –0.65 (–1.04 to –0.27; $p = 0.002$), whereas NF_{Cs}/NF_K did not change (+0.01; –0.41 to +0.43; $p = 0.96$; Fig. 7e, f). The slopes add up (–0.65 + 0.01 = –0.64). The LF ratio slope did not differ clearly from its permutation null (–1.00; $p = 0.07$), whereas the flat NF ratio differs from the slope of –0.35 expected if the caesium-to-potassium ratio of the plants were unrelated to that of the solutions (permutation range –0.65 to –0.05; $p = 0.015$, $q = 0.04$). Because the sediment $^{137}Cs/^{40}K$ ratio was almost collinear with sediment ^{137}Cs ($r = 0.96$, VIF 13) and the LF ratio contains sediment potassium in its numerator, the partial effect of potassium cannot be separated from ratio coupling. Counting errors did not affect these slopes ($\kappa = 0.99$).

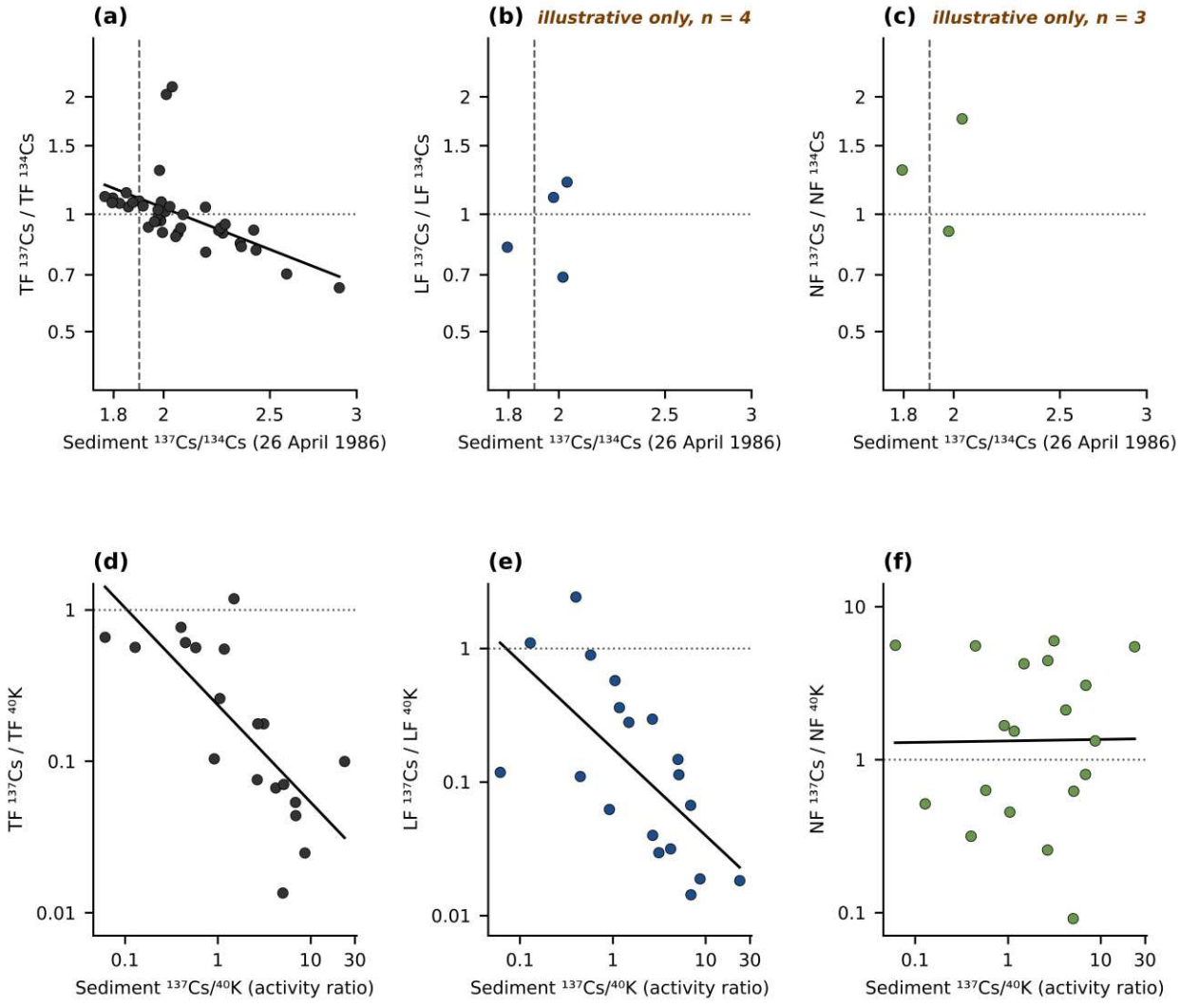


Fig. 7 Quotients of the transfer steps for two nuclides against the corresponding sediment quotient. Top, ^{137}Cs over ^{134}Cs against the sediment ^{137}Cs/^{134}Cs activity ratio R (decay-corrected to 26 April 1986; dashed vertical line, 1.90, Chernobyl deposition; ratios above it contain weapons-test ^{137}Cs): (a) TF_{137}/TF_{134}, n = 38, least-squares line; a slope of –1 is expected both if the plant ratio is unrelated to the sediment ratio and if weapons-test caesium is completely unavailable; (b) LF_{137}/LF_{134}, illustrative only, n = 4; (c) NF_{137}/NF_{134}, illustrative only, n = 3 (no lines fitted, no inference). Bottom, ^{137}Cs over ^{40}K against the sediment ^{137}Cs/^{40}K activity ratio at the 19 site-seasons with all four factors: (d) TF_{Cs}/TF_{K}, (e) LF_{Cs}/LF_{K}, (f) NF_{Cs}/NF_{K}, least-squares lines; the slopes add up ((e) + (f) = (d)). Dotted lines mark a quotient of one. Statistics, permutation null values and q values in Table S3. Abbreviations as in Fig. 1

3.5 How robust is the decline of LF?

Extreme thirds. Fig. 8 shows the additivity as chains. Between the lowest third of the site-seasons (n = 10; sediment 34–342 Bq kg^{-1}) and the highest third (n = 10; 2317–14 481 Bq kg^{-1}), the geometric mean of TF fell by 0.90 log units. This fall is the sum of 0.57 in log LF (from 0.72% to 0.20%) and 0.34 in log NF (from 126 to 58); the middle third lay in between (LF 0.27%, NF 78). The medians showed the same pattern (LF 0.80% and 0.20%, NF 140 and 51, TF 0.81 and 0.14); being medians of different site-seasons, they do not add up exactly. The per-decade values in Fig. 8 (–0.38 for LF, –0.22 for NF) are two-group contrasts of the extreme thirds and therefore differ from the regression slopes, which use all site-seasons.

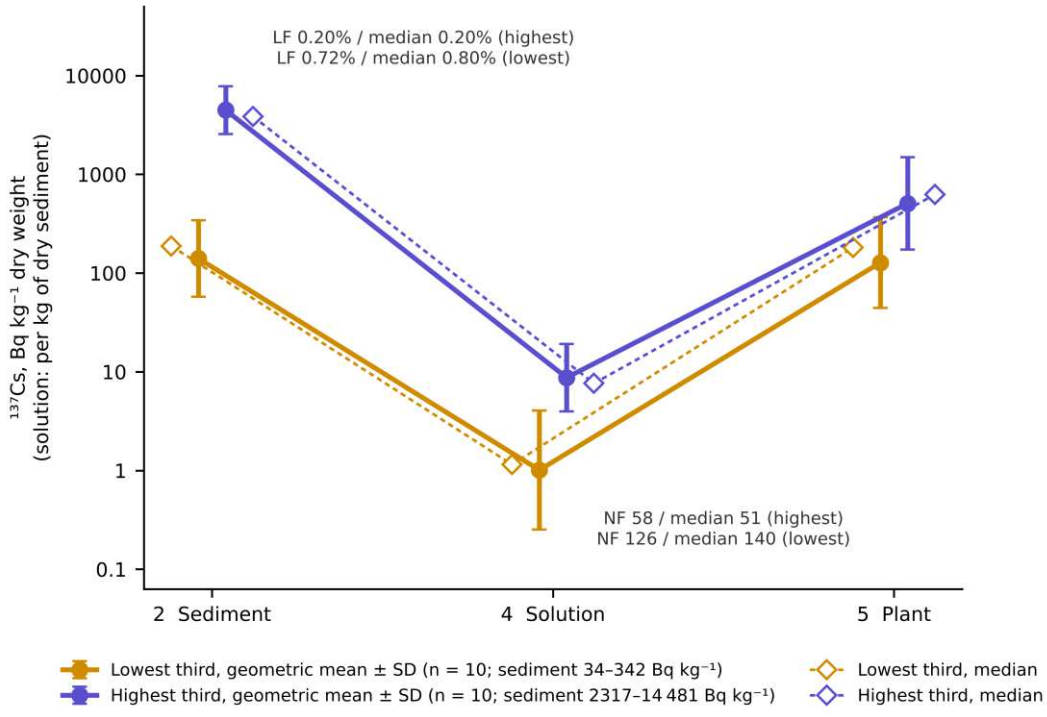


Fig. 8 Chains sediment (station 2) → solution (4) → plant (5) of ^{137}Cs for the lowest and the highest third of the 32 site-seasons ranked by sediment activity: geometric means ± one standard deviation of the logarithms (filled circles, solid lines) and medians (open diamonds, dashed lines); plant = median of the site-season. The drop from sediment to solution is log LF, the rise from solution to plant log NF; for the geometric means their sum is log TF, whereas medians of the three stations need not add up. Between the highest and the lowest third (geometric means), Δlog TF –0.90 = Δlog LF –0.57 + Δlog NF –0.34; per decade of sediment activity, TF –0.60 = LF –0.38 + NF –0.22. These per-decade values are contrasts between the two extreme thirds divided by their difference in log sediment activity; they differ from the regression slopes of Fig. 4, which use all site-seasons. Solution activities are expressed per kg of dry sediment. Abbreviations as in Fig. 1

Influence. Removing the least contaminated site-season steepened the LF slope to –0.45 ($p < 0.001$), and removing the three least contaminated (ha autumn, tr autumn, ri summer) gave –0.31 ($p = 0.024$). Leave-one-out slopes ranged from –0.44 to –0.27, with the largest $p = 0.018$. Removing four or more of the least contaminated site-seasons weakened the slope further (four: –0.29, $p = 0.052$; six: –0.16, $p = 0.29$). Removing up to seven of the most contaminated site-seasons left the slope between –0.36 and –0.42 ($p \leq 0.012$).

Censoring. The solutions with an estimated counting error above 30% belonged to the less contaminated sediments (mean log $C_{sediment}$ 2.4 against 3.2; Fig. 9a). Excluding them gave a steeper slope (–0.65, $p < 0.001$, $n = 24$), and error weighting gave –0.44. Treating them as upper limits in the Tobit model, however, gave –0.15. With thresholds of 40% and 50% (4 and 2 censored values) the Tobit slope was –0.28 and –0.33. On the more probable wet-sediment basis, 28 of 34 values would be censored and the Tobit model is not identifiable; the data then cannot distinguish a decline of LF from censoring. The decline of LF therefore holds only if the weak solution values are unbiased. It vanishes if they are regarded as no more than upper limits.

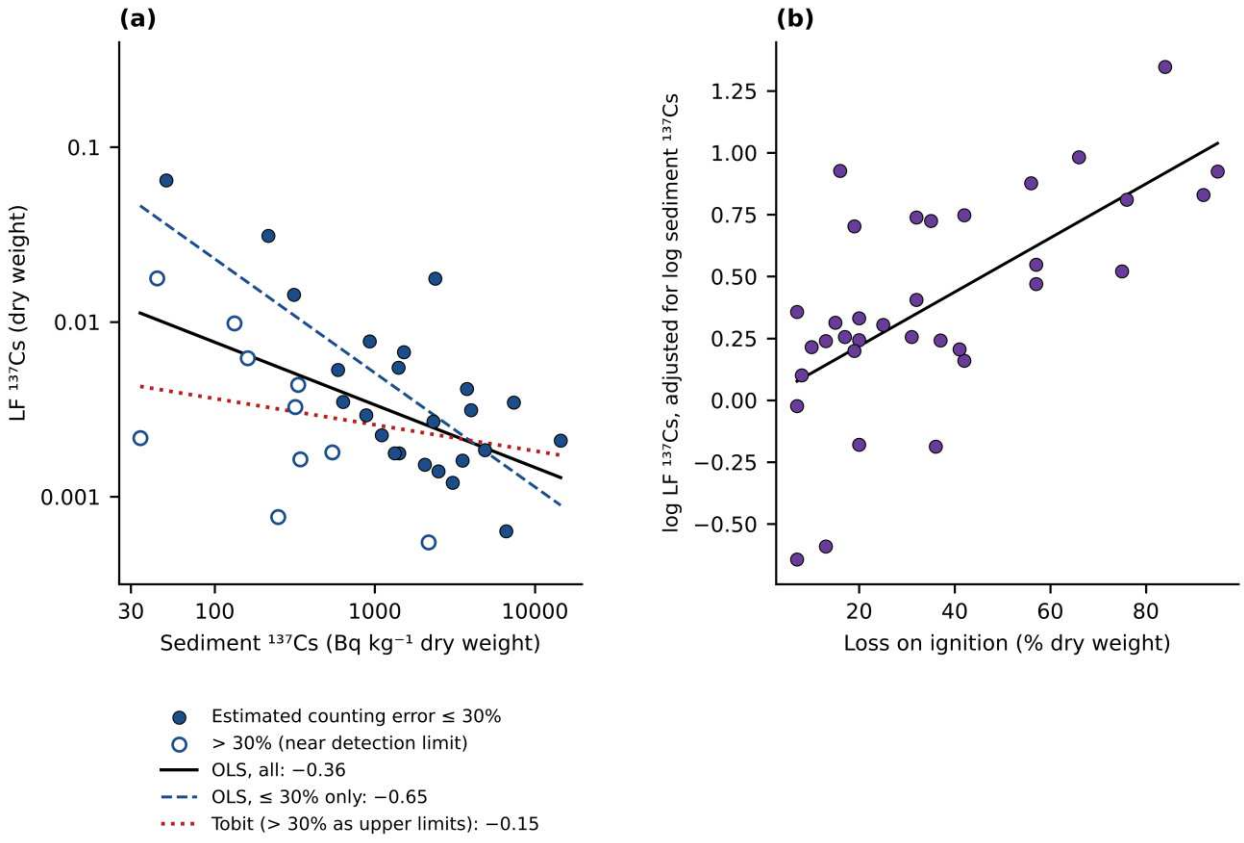


Fig. 9 Robustness of the decline of the solution factor LF of ^{137}Cs. (a) LF against sediment ^{137}Cs; open symbols mark solutions with an estimated counting error above 30% (near the detection limit; counting errors estimated from an error model of the same detector, assuming 30 g of dry sediment). Lines: least squares for all values and for the precise values only, and Tobit regression treating the imprecise values as upper limits. Without the three least contaminated site-seasons the OLS slope is –0.31 ($p = 0.02$). (b) Partial effect of loss on ignition (LOI) in the joint model log LF = a + b log $C_{sediment}$ + c LOI ($n = 34$): LOI +0.011 per % ($p < 0.001$), $C_{sediment}$ –0.58; VIF, variance inflation factor, 1.38. Abbreviations as in Fig. 1

Coupling. If the solution activities were unrelated to the sediment, the LF slope would be –1.00 (permutation 95% range –1.29 to –0.69); the observed –0.36 shows that the desorbed activity follows the sediment closely, though sub-proportionally. Random counting errors of the magnitudes estimated in Section 2.2, applied to a constant LF, gave a slope of 0.00 (95% range –0.11 to +0.10). Unbiased counting noise therefore cannot create the decline; a bias near the detection limit could. LF and NF were negatively correlated (r = –0.42), but less so than expected from their shared solution term alone (permutation null –0.78, 95% range –0.85 to –0.68). The variance of log TF (0.29) was therefore similar to that of log NF (0.28) and larger than that of log LF (0.22).

Grab-sample error. With σ_u = 0.32 (κ = 0.77), the corrected TF slope was –0.43. Under assumption A (LF unaffected) the corrected NF slope was –0.03; under assumption B the corrected LF slope was –0.50 and the NF slope +0.08. Propagating the uncertainty of σ_u gave a corrected NF slope of 0.00 (95% CI –0.47 to +0.52) under A, and slopes of –0.54 (–1.27 to –0.15) for LF and +0.13 (–0.38 to +1.20) for NF under B. SIMEX gave –0.06 (σ_u = 0.32) and 0.00 (σ_u = 0.41) for NF under A. An aliquot error of 0.1–0.2 log units left the expected LF slope unchanged (–0.36) and widened its spread only by about ±0.05 to ±0.11. After correction for sampling error, the NF slope is thus centred near zero, but its uncertainty spans a decline as steep as that of LF.

Excluded values. Reinstating the suspect pa summer solution as stored gave an LF slope of –0.32 (p = 0.019; Tobit –0.07), an LF ratio of potassium to caesium of 7.0 and an NF ratio of caesium to potassium of 0.99; with the decimal reading (21.3 Bq kg^{-1}) the LF slope was –0.34 (p = 0.004). Reinstating the invalid pu ^{40}K value raised the LF ratio of potassium to caesium to 8.8 (n = 21). Including the probably dead plants lowered the median NF of ^{137}Cs to 53 and the GM of TF to 0.33 (n = 123) and gave slopes of –0.58 for TF, –0.37 for LF and –0.21 for NF (33 site-seasons). None of these choices changed a conclusion (Table S1).

3.6 Sediment properties and the solution step

Sediment ^{137}Cs was correlated with loss on ignition (ρ = 0.59, p < 0.001) and with dry matter (ρ = –0.46, p = 0.013). In the joint model, LF rose with loss on ignition by 0.011 log units per percentage point (95% CI 0.005–0.016; p < 0.001; n = 34), and the coefficient of log $C_{sediment}$ became steeper (–0.58; 95% CI –0.80 to –0.37; VIF 1.38; R^2 = 0.51; Fig. 9b). Dry matter acted in the same way (–0.013 per percentage point, p = 0.024; $C_{sediment}$ –0.66; n = 28). Organic matter therefore does not explain the decline. It acted as a suppressor: the more contaminated sediments were more organic, and organic sediments released more caesium. Grain size did not modify the

slope. At the water-body level (n = 17), with the median grain size, the fraction < 0.5 µm or the fraction < 2 µm as covariate, the $C_{sediment}$ coefficient stayed between –0.42 and –0.51 and the grain-size terms had $p \geq 0.26$.

Montmorillonite in the clay fraction gave, at the water-body level, log LF = –1.02 – 0.53 log $C_{sediment}$ – 0.19 log montmorillonite ($R^2 = 0.42$; n = 17). The montmorillonite term had p = 0.24 and a bootstrap CI that included zero (–0.47 to +0.10). Counted per site-season, as in 1991, where the copied mineral values enter twice, it was –0.16 (p = 0.21; n = 24); with the stored pa summer value it was –0.32 (p = 0.053; n = 25), the value of the 1991 regression. Because ten mineral and particle-size descriptors were tested, a p value near 0.05 for one of them is expected by chance alone. In the screen of 17 descriptors (Table 3), no test reached a false-discovery rate below 0.05. The strongest was loss on ignition after adjustment for contamination ($\rho = +0.50$, p = 0.003, q = 0.09), and montmorillonite had $q \geq 0.76$. The 1991 regression with montmorillonite is therefore not confirmed as an effect.

The geology of the catchments did not explain LF either. Montmorillonite differed between geological classes (Kruskal–Wallis p = 0.010; means 5.5% in Neogene basins, 4.1% in Quaternary deposits, 0.9% in carbonate and 0.4% in crystalline catchments; 18 water bodies), but muscovite did not (p = 0.60), so that geology cannot stand in for the micaceous minerals. The five water bodies with carbonate catchments had a 2.7 times lower LF (Mann–Whitney p = 0.037; q = 0.57 in the screen), but all lie in the Enns and Palten valleys, the region of highest deposition; with this region as a covariate the difference was not significant (×0.44, p = 0.31), and at a given sediment activity it vanished (×0.86, p = 0.81). Catchment area (1–2327 ha) was unrelated to LF, NF or sediment ^{137}Cs ($|\rho| \leq 0.22$).

Table 3 Spearman correlations of sediment and catchment descriptors with LF of ^{137}Cs, ordered by decreasing explanatory strength (|ρ adjusted|, ties by |ρ direct|), directly and after removing the dependence on log sediment ^{137}Cs (adjusted), with false-discovery-rate q values (Benjamini–Hochberg over all 34 tests). Descriptors determined once per water body (minerals, grain size, altitude, catchment) are tested at the water-body level (mean log LF and mean log sediment ^{137}Cs of its site-seasons); the others per site-season. Mineral contents are relative contents of the clay fraction (< 2 µm); carbonate catchment after the Geological Map of Styria. Abbreviations as in Fig. 1

Descriptor	Level	n	ρ direct	p	q	ρ adjusted	p	q
loss on ignition	site-season	34	+0.16	0.358	1.00	+0.50	0.003	0.09
montmorillonite	water body	17	–0.13	0.620	1.00	–0.38	0.134	0.76
dry matter	site-season	28	–0.03	0.875	1.00	–0.34	0.079	0.76
quartz	water body	17	–0.38	0.130	0.76	–0.30	0.235	0.89
altitude	water body	23	+0.09	0.680	1.00	+0.29	0.175	0.78
muscovite	water body	17	–0.42	0.094	0.76	–0.26	0.321	0.99
clay minerals (sum)	water body	17	–0.18	0.498	1.00	–0.19	0.474	1.00
amorphous	water body	17	+0.34	0.184	0.78	+0.18	0.491	1.00

fraction < 0.5 µm	water body	17	+0.18	0.483	1.00	–0.12	0.637	1.00
fraction < 2 µm	water body	17	+0.11	0.673	1.00	–0.12	0.639	1.00
sediment ^{40}K	site-season	27	–0.05	0.823	1.00	–0.09	0.661	1.00
carbonate catchment (1/0)	water body	23	–0.44	0.033	0.57	–0.08	0.719	1.00
kaolinite	water body	17	–0.05	0.840	1.00	–0.04	0.869	1.00
catchment area	water body	23	–0.22	0.321	0.99	–0.03	0.879	1.00
pH (KCl)	site-season	33	+0.02	0.911	1.00	+0.03	0.871	1.00
median grain size	water body	17	–0.01	0.981	1.00	–0.02	0.937	1.00
chlorite	water body	17	–0.21	0.421	1.00	–0.00	0.996	1.00

3.7 Sediment and riparian soil

At the site level, sediment ^{137}Cs was only loosely related to ^{137}Cs in the upper 5 cm of the riparian soil ($r = 0.36$, $p = 0.12$; $\rho = 0.36$; $n = 20$ water bodies; Fig. 10). Restricted to the 17 water bodies with a bank sample of their own, the values were $r = 0.40$ and $\rho = 0.43$ ($p = 0.09$). The sediment-to-soil ratio had a GM of 0.64 (median 0.87) and ranged from 0.03 (ri) to 5.6 (pu). Sites at which the sediment had accumulated more caesium relative to the soil had lower LF ($\rho = –0.57$, $p = 0.009$). Because the ratio and LF share $C_{sediment}$, however, a correlation of –0.37 (95% range –0.59 to –0.15) is expected when the soil values are shuffled. The observed value exceeds this only marginally (permutation $p = 0.04$). At a given sediment activity, LF tended to rise with soil activity ($\rho = +0.39$, $p = 0.09$). How much of the regional fallout the sediments retained, the first step of the two-step model of 1989, is analysed in Ahamer (in preparation).

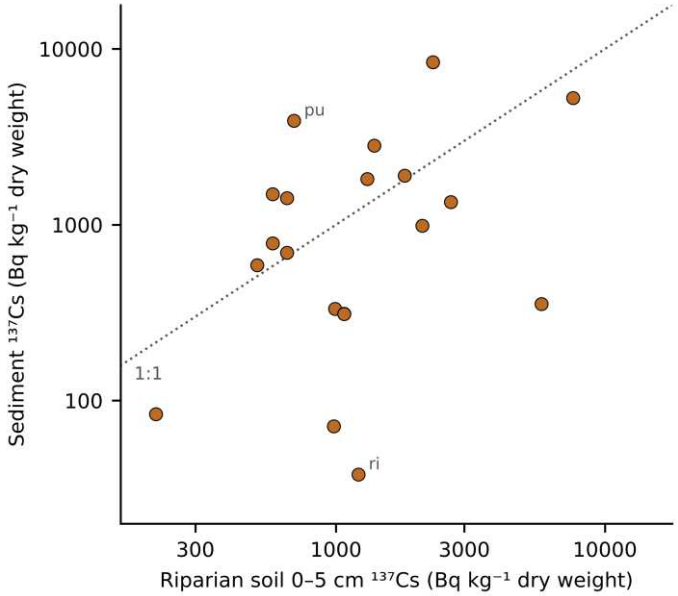


Fig. 10 ^{137}Cs in the sediment against ^{137}Cs in the 0–5 cm layer of the adjacent riparian soil at the site level (geometric means over seasons, season duplicates of the soil values removed; dry weight, decay-corrected to 26

April 1986); dotted line 1:1. The sites with the lowest and highest sediment-to-soil ratio are labelled (ri, pu); r, Pearson correlation of the logarithms; ρ, Spearman rank correlation: r = 0.36 (p = 0.12), ρ = 0.36, n = 20 sites

4. Discussion

4.1 Potassium leaves, caesium stays

The eightfold difference in desorbability runs against the history of the two elements. Potassium has been part of the sediment minerals since their formation, much of it in mica and feldspar lattices. The Chernobyl caesium, in contrast, had been in the sediments for about one and a half years when they were sampled. The 1991 report already noted that a potassium atom was about ten times more likely to be desorbed than a caesium atom [30, p. 94]; with the present CI the factor lies between about 4 and 15. The explanation lies in the selectivity of the sorption sites. Frayed-edge and wedge sites of illite and mica bind caesium several orders of magnitude more selectively than potassium [7, 9, 10, 55]. Sorption on them is only partly reversible [56, 57], the collapse of illite interlayers traps caesium further [58], and much fresh caesium is fixed within months [59, 60]. Even in a dilute KCl medium with a caesium sink, desorption of ^{137}Cs from Fukushima soils continued for months, and stable caesium was released much less than ^{137}Cs [61]. A 24-h test therefore captures mainly the rapidly exchangeable pool. The low LF values are consistent with distribution coefficients of radiocaesium of the order of 10^3 L kg^{-1} in mineral soils [62, 63], and the same selective retention governed caesium mobility after Fukushima [64, 65].

Kd values of caesium depend on the experimental approach and duration [66] and, in sediments, on temperature, particularly where hydroxy-aluminium interlayers occur in 2:1 clay minerals [67]; the temperature of the shaking test was not recorded. LF is therefore an operational index, comparable between the sites of this survey because all sediments were treated alike, not a transferable distribution coefficient.

The decomposition places the contrast between the elements in the solution step: the LF ratio (0.12) accounts for the whole TF ratio (0.17), and the NF ratio is not distinguishable from one. This is not the same as saying that the plants did not discriminate. First, equality is shown only within a factor of about two. In solution culture, roots absorbed potassium about twice as rapidly as caesium relative to their concentrations [68], a difference of the size that the present NF ratio could not detect. Second, NF of potassium is not a physiological uptake coefficient: plants regulate their potassium, and on the same data plant K was unrelated to solution K (r = –0.11; Ahamer, in preparation). NF_K therefore mainly mirrors the solution K, and the near-equality of the median NF of the two elements may partly be coincidental. Third, the solution is a salt

extract expressed per kilogram of sediment, not a pore-water concentration, so root selectivity cannot be read from it. The robust statement is therefore narrower. TF of caesium was about four times lower than that of potassium, and this contrast arose where caesium had to leave the sediment; no additional contrast was detectable between solution and plant. Stable-element analyses of two *Carex rostrata* samples in the 1991 report point the same way, with plant-to-sediment ratios about 16 times higher for potassium than for caesium [30, p. 28]. Where more potassium was desorbed, NF of caesium was lower ($r = –0.61$, $p = 0.006$, $n = 19$; partial coefficient –0.48, $p = 0.018$, after adjustment for LF of caesium). This agrees with the dependence of caesium uptake on the accompanying cations K^+, Na^+ and NH_4^+ [69, 70], with the competition of potassium and caesium at the root [4, 17, 71] and with that in freshwater fish [72, 73]. Both quantities share the solution measurement, however, so part of the correlation may be methodological.

4.2 Alternative interpretations of the declining solution factor

The original interpretation [29, 31] attributed the sub-proportional transfer to the sediment. The present data support a decline of LF with contamination, but several mechanisms could produce it, and not all are physical (Table 4).

Table 4 Alternative explanations for the decline of the solution factor LF of ^{137}Cs with sediment activity, the tests possible with the survey data and their outcome (details in Sections 3.5–3.7 and 4.2)

Alternative mechanism	Test with the present data	Result (LF slope or statistic)	Assessment
(a) Censoring / bias of weak solutions near the detection limit	Exclusion, weighting and Tobit regression of values with estimated counting error > 30%	–0.65 / –0.44 / –0.15	Not excluded; decisive (wet basis: not identifiable)
(b) Organic matter or dry-weight normalisation	Joint models with loss on ignition, dry matter (VIF)	$C_{sediment}$ –0.58 with LOI; –0.66 with dry matter	Rejected as explanation (suppressor)
(c) Focusing of fine, already bound particles; redistribution	Grain-size covariates; sediment/soil ratio with permutation null	Grain size $p \geq 0.26$; ratio ρ –0.57 vs null –0.37	Not supported, not excluded
(d) NH_4^+/K^+ status of pore water	No data (not measured in 1987)	–	Open
(e) Non-linear sorption (site saturation)	Trace loadings; relation is between sites	–	Unlikely
(f) Ageing, storage (drying, NH_4^+ release)	Same deposition date; storage not documented	–	Unlikely to depend on contamination
(g) Aliquot heterogeneity (30 g vs 1-L beaker)	Simulation, σ = 0.1–0.2 log units	Mean slope –0.36, no bias	Rejected as explanation

(a) Censoring near the detection limit. This is the most serious alternative. The weak solutions belonged to the least contaminated sediments. If such values were reported only when they exceeded a decision threshold, or were biased upwards near it, LF would be overestimated at low contamination, which is exactly the observed pattern. The data cannot exclude this: the

slope survives exclusion or down-weighting of the weak values (–0.65, –0.44) but is reduced to –0.15 when they are treated as upper limits. The 1991 counting errors and decision thresholds [36] would settle the question; they were never recorded. If, as is more probable, the 30 g of sediment refer to wet mass, most solutions lie near detection and the question cannot be settled with these data.

(b) Organic matter or dry-weight normalisation. More contaminated sediments were more organic, so a dry-weight artefact or an organic-matter effect could in principle mimic a contamination effect. The joint models show the opposite: adjusting for loss on ignition or dry matter steepened the slope. The positive organic-matter effect agrees with the high transfer from organic soils [26, 63, 74] and with the finding that incorporating organic matter into soils changed the ^{137}Cs uptake of wheat [75]. It also agrees with the finding that the organic sediments of Lake Vorsee did not follow the illite-based prediction of caesium partitioning that held for Lakes Constance and Lugano [76]. Distribution coefficients measured on mixtures of clay and humic material show that the organic component has to be considered together with the mineral one [77]: organic matter dilutes the selective mineral sites and can block caesium access to frayed edges [78].

(c) Redistribution and focusing of particle-bound caesium. Fine particles that had bound caesium in the catchment or the water column could accumulate in some sediments and raise their activity in a less exchangeable form [79]. Experiments with lake sediments indicated that caesium delivered on settling particles is held more strongly than caesium that diffuses across the sediment–water interface [80]. The test with grain size was negative, and the apparent link between the sediment-to-soil ratio and LF is largely the coupling through $C_{sediment}$ (Section 3.7). The hypothesis remains plausible but is not supported by these data.

(d) Ammonium and potassium in the pore water. NH_4^+ released by the mineralisation of organic matter mobilises caesium from frayed-edge sites in anoxic sediments [13, 14], and NH_4^+, K^+ and ^{137}Cs compete for the same exchange sites in soils [81]. In reservoirs after Fukushima, the sediment–pore-water Kd of ^{137}Cs decreased with increasing NH_4^+ [82], and NH_4^+ also modified dissolved caesium in ponds of the exclusion zone [83]. Pore-water chemistry was not measured in 1987. Moreover, 11–14 months of storage may have changed the NH_4^+ status of the sediments before the desorption test. If more contaminated sites were also less eutrophic, NH_4^+ could produce the pattern; this cannot be tested.

(e) Non-linear sorption. Selective sites saturate at high caesium loadings [84], but fallout caesium occupies only a minute fraction of them. Within one sediment, sorption at these trace levels is practically linear, so non-linearity cannot explain a relation between sites.

(f) Ageing and storage. Time since deposition was the same at all sites, so contamination-dependent ageing is unlikely unless caesium reached the sediments by different routes (see c). Drying or wet–dry cycles during storage increase fixation, but there is no reason why they should have acted differently at more contaminated sites.

(g) Aliquot heterogeneity. A 30 g aliquot that is not representative of the counted beaker adds noise to LF but no bias against the beaker activity (Section 3.5).

On balance, a physical decline of the desorbable fraction with contamination is consistent with the data and with the original interpretation. However, it is not established against the censoring explanation, and the mechanism (redistribution, organic matter, pore-water chemistry) remains open.

4.3 Which step carries the concentration dependence?

The re-examination of the transfer factors (Ahamer, submitted to J. Environ. Radioact.) concluded that the sub-proportional transfer most plausibly arises between sediment and water. The decomposition is consistent with this but gives a weaker answer than a single number suggests. Of the TF slope of –0.55, LF carries –0.39 and NF –0.16, with a bootstrap CI for the LF share of 19–129%. After correction for the grab-sample error, the NF slope is centred near zero (0.00 under assumption A, +0.13 under B), but its interval includes declines as steep as that of LF. Physiology leads one to expect a nearly constant NF. Radiocaesium is a tracer, and its uptake should be proportional to its concentration in solution at a ratio set by potassium, ammonium and stable caesium [4, 17]. Within the precision of the survey, the data do not contradict this expectation, but they do not prove it either. The chains in Fig. 8 show where the evidence is weakest: the largest steps of both LF and NF lie between the lowest third and the rest, and the lowest third is also the third with the weakest solutions. There, a censoring bias would raise LF and lower NF at the same time.

The conclusion is therefore conditional. If the weak solution values are unbiased, the solution step carries most of the concentration dependence of TF, and the remaining NF slope is compatible with sampling error. If they are biased high, the evidence for any step-specific concentration dependence disappears. The decline of TF itself remains (–0.51 over 39 site-seasons), and it holds for the Chernobyl ^{134}Cs alone (Section 4.4). In both cases, the potassium–caesium contrast is located in the solution step, because that result rests on the ratio of two solution values from the same extract and does not depend on the detection limit in the same way. The three-station model is thus, as the project report anticipated for its own model,

preliminary: field data of this kind can locate a dependence but not establish its mechanism, which requires targeted laboratory tests under controlled conditions.

4.4 What the further decompositions add

Potassium-40. For potassium, the decomposition shows mainly the limits of the data. The steep decline of LF of ^{40}K lies within the range produced by ratio coupling over a fivefold range of sediment potassium, and the tendency of exchangeable potassium to be higher in organic, potassium-poor sediments did not survive correction for multiple testing; total ^{40}K resides mostly in mineral lattices and says little about the exchangeable pool. Plant potassium was nearly independent of solution potassium, as expected for plants that regulate their potassium, so that NF of ^{40}K mainly mirrors the solution and not a physiological coefficient; over the larger set of the companion paper, plant potassium tended to follow total rather than salt-exchangeable sediment potassium (Ahamer, in preparation). The shallow, non-significant decline of TF of ^{40}K (–0.53) is the net result of a nearly constant plant potassium over a narrow range of sediment potassium. ^{40}K therefore cannot serve as a simple analogue for the concentration dependence of caesium transfer; the solution step of potassium is dominated by the noise of low ^{40}K activities in the extracts and by ratio coupling.

Caesium-134. The decline of TF is not an artefact of mixing caesium of two ages. ^{134}Cs, which came from Chernobyl alone, showed a decline as steep as ^{137}Cs at the same site-seasons (–0.66 against –0.61) and clearly less steep than the null value. The sub-proportional transfer of TF is thus a property of the Chernobyl caesium itself. Because the solutions of 1988 contained a reported ^{134}Cs value at only four site-seasons, the data cannot tell whether the decline of ^{134}Cs, like that of ^{137}Cs, resides in the solution step.

Isotope ratio. The hypothesis that Chernobyl caesium was more readily desorbed and more available to plants than older weapons-test caesium is plausible: caesium becomes progressively fixed in the interlayers of micaceous minerals with time [57, 59, 60]. It is not testable with these data: they neither confirm nor exclude it. The two tests point in opposite directions. The level of the ratio speaks for equal availability: on average, plants contained the two sources in the proportion of their sediments ($TF_{137}/TF_{134} = 1.00$), and their mean isotope ratio exceeded that of Chernobyl deposition, so weapons-test caesium was not entirely unavailable. Its pattern across sites speaks for reduced availability: locally, the plant ratio did not follow the sediment ratio, which is what an unavailable weapons-test component would produce (slope –1). Sampling heterogeneity of the grab samples could produce the latter as well, because a grab sample need not have the isotope ratio of the root zone, and this representativeness error, unlike the counting

error, is not contained in κ. Expressed directly, the transfer of weapons-test caesium may lie anywhere between 0.28 and 2.7 times that of Chernobyl caesium. The weapons-test share (median 6%, or 10% with the release ratio of 1.82) is simply of the same order as the precision of the isotope ratio, half of whose variation between sediments is counting error. The four LF quotients (GM 0.93) point in the direction of the hypothesis, but they are illustrative only. The ratio NF_{137}/NF_{134}, which must be one for physical reasons, could be checked only at three site-seasons. A decisive test would require sediments with a larger weapons-test share and solutions counted well above their detection limits.

Caesium relative to potassium. The quotient view repeats the central finding in a form that does not depend on the activity level alone. Where the sediments carried more caesium relative to potassium, the plants received relatively less caesium, and this reduction arose entirely between sediment and solution, whereas the uptake step left the caesium-to-potassium ratio of the solution unchanged on average. Because the sediment ratio is dominated by ^{137}Cs, these panels are not independent evidence for the decline of LF; they add that the competition of potassium did not change the uptake step along the contamination gradient.

4.5 Sediment properties

Loss on ignition was the only sediment property with consistent support. The bulk mineral contents did not explain LF, for reasons that remain unknown. That the substrate mineral matters for caesium uptake was shown early: uptake differed between illite, kaolinite, montmorillonite and peat as the colloid [85], and different clay minerals changed caesium uptake by beans [86]. One plausible reason for the negative result is that exchangeability is controlled by a small number of highly selective sites that bulk mineral contents and grain-size fractions do not capture. The radiocaesium interception potential (RIP), which measures these sites, predicts the solid–liquid distribution of caesium in soils and sediments better than clay content [10, 11, 87] and varies over orders of magnitude between soils [88]. In 1987 the method had only just been published, and the survey did not include it. With only 17 water bodies with mineralogy, the power to detect a mineral effect was also small. The montmorillonite term of the 1991 regression is not supported at the water-body level or after correction for multiple testing. Its sign is also not what experiments lead one to expect: caesium sorption on montmorillonite was found reversible at all loadings, whereas on illite it became irreversible at high loadings [89]. Montmorillonite-rich sediments should therefore release caesium more readily, not less. The high caesium retention of the el sediment, rich in montmorillonite and muscovite [30, p. 90], is more plausibly a muscovite (micaceous) effect, although across the water bodies

muscovite explained neither LF nor the retention of fallout by the sediment (Ahamer, in preparation).

4.6 Water pathway and the ratio of caesium to potassium

The 1991 report divided uptake into a direct, a soil and a water pathway [30, p. 8]. The present decomposition cannot assess the water pathway. Only one water sample was measured, at el, with 0.19 Bq kg^{-1} (counting error 44%), about 10^{-4} of the sediment activity. Relative to this sample, plants of el in the same season contained 9–74 times the water activity per kg fresh weight for the submerged or floating *Potamogeton panormitanus*, *Hydrocharis morsus-ranae*, *Ceratophyllum demersum* and *Elodea canadensis*, and 118–919 times for the emergent and riparian *Juncus effusus*, *Lythrum salicaria*, *Carex rostrata* and *Alisma plantago-aquatica*; with a single water sample near detection, these concentration ratios indicate orders of magnitude only. Floating-leaved and submerged plants can take up caesium from the water column [90, 91]; in submerged Characeae, the Cs/K ratio of the medium governs the accumulation of ^{137}Cs [92]. The solution of the shaking test is an operational model of the exchangeable sediment pool, not of the open water.

The ratio of caesium to potassium activity in the plants indicates the additional radiation from the accident relative to the natural ^{40}K [30, p. 92]. At the time of measurement, ^{137}Cs + ^{134}Cs had a median of 0.38 times the ^{40}K activity (interquartile range 0.17–0.83) and exceeded it in 23% of the samples. Since the caesium–potassium contrast arose in the solution step, it was the selective retention of caesium in the sediments that kept this ratio low.

4.7 Limitations

- The reagent (most probably $CaCl_2$), its concentration, the liquid-to-solid ratio, the phase separation, the blank, the temperature and the storage of the sediments are not documented.
- The test was carried out 11–14 months after sampling, at one solid-to-solution ratio and without replicates.
- The counting errors of the solutions were never recorded and had to be estimated; the central LF slope is sensitive to how values near detection are treated.
- LF exists once per site-season, so its within-site variability is unknown.
- For ^{40}K and ^{134}Cs the numbers of LF values are small (25 and 4), the range of sediment ^{40}K is narrow, and one ^{137}Cs value (pa, summer) is probably a decimal error (Section 3.1).
- The weapons-test share of the sediment ^{137}Cs (median 6%; 10% with a Chernobyl ratio of 1.82 instead of 1.90) is of the order of the counting precision of the isotope ratio.

- The decompositions of Section 3.4 are exploratory; several of their nominal p values do not survive correction for multiple testing.
- The mineral contents are relative values of the clay fraction, available for 17 of the 23 water bodies with LF.
- The acid-extract station was not used here; the three-station model treats the sediment as one pool.

5. Conclusions

(1) One year after Chernobyl, a median of 0.3% of the ^{137}Cs in Styrian pond sediments was exchangeable with a dilute salt solution, whereas potassium was released about 4–15 times more readily. The absolute values are specific to the desorption test.

(2) TF of caesium was about four times lower than that of potassium. This contrast arose in the sediment–solution step; between solution and plant, no difference between the elements was detectable (ratio 1.04, 95% CI 0.48–1.83).

(3) On logarithmic scales the steps of the three-station model and their slopes against contamination add up to those of TF. The decline of TF (–0.55) split into –0.39 for LF and –0.16 for NF. The LF share is uncertain (19–129%), and the decline of LF holds only if the weak solution values are unbiased.

(4) The decline of TF holds for ^{134}Cs, that is, for Chernobyl caesium alone (slope –0.66). On average the plants contained the two caesium sources in the proportion of their sediments, but locally they did not follow the sediment isotope ratio; with a weapons-test share of 6%, the relative availability of weapons-test caesium remains undetermined (0.28–2.7). The decline of TF_{Cs}/TF_K with the sediment ^{137}Cs/^{40}K ratio arose entirely in the solution step.

(5) Organic matter raised LF at a given contamination and did not explain its decline; no mineralogical or geological effect survived analysis at the water-body level and correction for multiple testing.

(6) Desorption tests intended to locate the concentration dependence of transfer should report counting errors and decision thresholds, the reagent and blank, and the storage of the samples. This is the targeted laboratory test that the project report of 1991 named as the next step for its preliminary model [30, p. 7].

Supplementary Information

Supplementary Information: Table S1 (sensitivity of the main results to the excluded values), Table S2 (site-season values of LF, NF and TF), Table S3 (statistics of the decompositions for ^{40}K, ^{134}Cs and the quotients $^{137}Cs/^{134}Cs$ and $^{137}Cs/^{40}K$, with false-discovery-rate q values).

Acknowledgements

The author thanks the late Prof. Hansjörg Müller (Reactor Institute Graz, Graz University of Technology), in whose laboratory the gamma-spectrometric measurements were made, and the late Prof. Georg Heinrich (Institute of Plant Physiology, University of Graz; plant metabolism and systematics) for making the original study possible; H. Kolmer and K. Klima (Institute of Mineralogy and Technical Geology, Graz University of Technology) for the particle-size and X-ray analyses; Prof. Othmar Nestroy for advice on soil science; W. Wegscheider and M. Maichin (Institute of Micro- and Radiochemistry, Graz University of Technology) for the atomic spectrometric determination of stable potassium and caesium; the late Prof. Josef Gölles (Institute of Electronic Data Processing, Graz) for advice on the correlation analysis of about 2600 data; the UBIS office of Graz University Library and the Austrian Research Centre Seibersdorf for literature searches; K. Oswald and F. Pacher for help with measurements and mineralogical analyses; and the staff of the Reactor Institute Graz, including colleagues S. Meisel and C. Zeck.

Declarations

Funding

No funding was received for conducting this study.

Competing interests

The author has no competing interests to declare that are relevant to the content of this article.

Data availability

The original data files (Statgraphics, state of 12 May 1991), the derived tables and the analysis scripts of this paper are available in Zenodo, version 3 (DOI https://doi.org/10.5281/zenodo.23898698) [93].

Code availability

The analysis scripts (Python 3) are part of the Zenodo data set [93].

Author contributions

Gilbert Ahamer is the sole author. He designed the field and laboratory programme of 1987–1991, carried out the sampling and the evaluation of 1988–1991, re-analysed the data and wrote the manuscript.

Ethics approval

Not applicable.

Use of generative AI

The research questions, the field and laboratory programme of 1987–1991 including the desorption experiments, the original database, the decomposition of the transfer factor into solution and nutrition factors and its interpretation are the author's own long-term work. During the preparation of this work the author used Claude (Anthropic) to decode the archived data files, re-run the statistical analyses, draft figures and improve the language. After using this tool, the author reviewed and edited the content as needed and takes full responsibility for the content of the publication.

References

1. IAEA (2010) Handbook of Parameter Values for the Prediction of Radionuclide Transfer in Terrestrial and Freshwater Environments. Technical Reports Series No. 472. International Atomic Energy Agency, Vienna.
2. Menzel RG (1965) Soil–plant relationships of radioactive elements. Health Phys 11:1325–1332. https://doi.org/10.1097/00004032-196512000-00009
3. Pally M, Foulquier L (1981) Synthèse bibliographique sur la fixation du radiocésium par les végétaux aquatiques [Bibliographic synthesis on the uptake of radiocaesium by aquatic plants]. Report CEA-BIB-235, Commissariat à l'Énergie Atomique, Centre d'Études Nucléaires de Cadarache.
4. Zhu YG, Smolders E (2000) Plant uptake of radiocaesium: a review of mechanisms, regulation and application. J Exp Bot 51:1635–1645. https://doi.org/10.1093/jexbot/51.351.1635
5. White PJ, Broadley MR (2000) Mechanisms of caesium uptake by plants. New Phytol 147:241–256. https://doi.org/10.1046/j.1469-8137.2000.00704.x
6. Tamura T, Jacobs DG (1960) Structural implications in cesium sorption. Health Phys 2:391–398. https://doi.org/10.1097/00004032-195910000-00009
7. Evans EJ, Dekker AJ (1966a) Fixation and release of cesium-137 in soils and soil separates. Can J Soil Sci 46:217–222. https://doi.org/10.4141/cjss66-035
8. Sawhney BL (1972) Selective sorption and fixation of cations by clay minerals: a review. Clays Clay Miner 20:93–100. https://doi.org/10.1346/CCMN.1972.0200208
9. Eberl DD (1980) Alkali cation selectivity and fixation by clay minerals. Clays Clay Miner 28:161–172. https://doi.org/10.1346/CCMN.1980.0280301
10. Cremers A, Elsen A, De Preter P, Maes A (1988) Quantitative analysis of radiocaesium retention in soils. Nature 335:247–249. https://doi.org/10.1038/335247a0

11. Wauters J, Elsen A, Cremers A, Konoplev AV, Bulgakov AA, Comans RNJ (1996) Prediction of solid/liquid distribution coefficients of radiocaesium in soils and sediments. Part one: a simplified procedure for the solid phase characterisation. Appl Geochem 11:589–594. https://doi.org/10.1016/0883-2927(96)00027-3
12. Francis CW, Brinkley FS (1976) Preferential adsorption of ^{137}Cs to micaceous minerals in contaminated freshwater sediment. Nature 260:511–513. https://doi.org/10.1038/260511a0
13. Evans DW, Alberts JJ, Clark RA (1983) Reversible ion-exchange fixation of cesium-137 leading to mobilization from reservoir sediments. Geochim Cosmochim Acta 47:1041–1049. https://doi.org/10.1016/0016-7037(83)90234-X
14. Comans RNJ, Middelburg JJ, Zonderhuis J, Woittiez JRW, De Lange GJ, Das HA, Van Der Weijden CH (1989) Mobilization of radiocaesium in pore water of lake sediments. Nature 339:367–369. https://doi.org/10.1038/339367a0
15. Smith JT, Comans RNJ, Elder DG (1999) Radiocaesium removal from European lakes and reservoirs: key processes determined from 16 Chernobyl-contaminated lakes. Water Res 33:3762–3774. https://doi.org/10.1016/S0043-1354(99)00087-1
16. Smith JT, Beresford NA (2005) Chernobyl – Catastrophe and Consequences. Springer-Praxis, Berlin, Chichester. https://doi.org/10.1007/3-540-28079-0
17. Smolders E, Van den Brande K, Merckx R (1997) Concentrations of ^{137}Cs and K in soil solution predict the plant availability of ^{137}Cs in soils. Environ Sci Technol 31:3432–3438. https://doi.org/10.1021/es970113r
18. Nishita H, Romney EM, Alexander GV, Larson KH (1960) Influence of K and Cs on release of Cs^{137} from three soils. Soil Sci 89:167–176. https://doi.org/10.1097/00010694-196003000-00007
19. Evans EJ, Dekker AJ (1966b) Plant uptake of Cs-137 from nine Canadian soils. Can J Soil Sci 46:167–176. https://doi.org/10.4141/cjss66-027
20. Dafydd C, Prime D (1983) Desorption behaviour of artificial radionuclides sorbed on to estuarine silt: (I) caesium-137 and ruthenium-106, (II) zirconium-95 and niobium-95. Environ Pollut Ser B 5:273–295. https://doi.org/10.1016/0143-148X(83)90022-8
21. Konoplev AV, Bulgakov AA, Popov VE, Bobovnikova TsI (1992) Behaviour of long-lived Chernobyl radionuclides in a soil–water system. Analyst 117:1041–1047. https://doi.org/10.1039/AN9921701041
22. Sheppard MI (1985) Radionuclide partitioning coefficients in soils and plants and their correlation. Health Phys 49:106–111.
23. Kühn W, Handl J, Schuller P (1984) The influence of soil parameters on $^{137}Cs^{+}$-uptake by plants from long-term fallout on forest clearings and grassland. Health Phys 46:1083–1093. https://doi.org/10.1097/00004032-198405000-00008
24. Kerpen W (1986) Bioavailability of the radionuclides ^{137}Cs, ^{60}Co, ^{54}Mn and ^{85}Sr in various soils as a function of soil properties, in: Sibley, T.H., Myttenaere, C. (Eds.), Application of Distribution Coefficients to Radiological Assessment Models. Elsevier Applied Science, London, pp. 322–335.
25. Absalom JP, Young SD, Crout NMJ, Nisbet AF, Woodman RFM, Smolders E, Gillett AG (1999) Predicting soil to plant transfer of radiocesium using soil characteristics. Environ Sci Technol 33:1218–1223. https://doi.org/10.1021/es9808853
26. Absalom JP, Young SD, Crout NMJ, Sanchez A, Wright SM, Smolders E, Nisbet AF, Gillett AG (2001) Predicting the transfer of radiocaesium from organic soils to plants using soil characteristics. J Environ Radioact 52:31–43. https://doi.org/10.1016/S0265-931X(00)00098-9
27. Almahayni T, Beresford NA, Crout NMJ, Sweeck L (2019) Fit-for-purpose modelling of radiocaesium soil-to-plant transfer for nuclear emergencies: a review. J Environ Radioact 201:58–66. https://doi.org/10.1016/j.jenvrad.2019.01.006

28. Ahamer G, Müller H, Oswald K, Heinrich G, Kolmer H, Klima K, Pacher F (1989) The uptake of radioactive cesium into the aquatic vegetation of Styria/Austria, in: Proceedings of the XIX Annual Meeting of the European Society for New Methods in Agricultural Research (ESNA), Vienna, 29 August – 2 September 1988. Report OEFZS-4489, Austrian Research Centre Seibersdorf, pp. 157–181. https://www.researchgate.net/publication/263205370
29. Ahamer G, Müller H, Heinrich G (1992) Wieviel radioaktives Cäsium enthalten Pflanzen und Sedimente in steirischen Gewässern? [How much radioactive caesium is contained in plants and sediments of Styrian waters?] Mitt Naturwiss Ver Steiermark 122:5–18. https://www.zobodat.at/pdf/MittNatVerSt_122_0005-0018.pdf
30. Ahamer G (1991) Die Aufnahme von radioaktivem Cäsium in die Teichvegetation der Steiermark – Messungen und Modellerstellungen. Arbeitsbericht über Untersuchungen samt Literaturstudie, Band 1: Darstellung der Ergebnisse [The uptake of radioactive caesium into the pond vegetation of Styria – measurements and models. Final report]. Institute of Theoretical Physics, Graz University of Technology, and Reactor Institute Graz, Graz. https://www.researchgate.net/publication/318827375
31. Ahamer G (2012) Geo-referenceable model for the transfer of radioactive fallout from sediments to plants. Water Air Soil Pollut 223:2511–2524. https://doi.org/10.1007/s11270-011-1044-x Available as https://www.researchgate.net/publication/236605047
32. Ahamer G, Müller H (1993) Überlegungen für ein Modell zum Verhalten von radioaktivem Cäsium in der Teichvegetation [Considerations for a model of the behaviour of radioactive caesium in pond vegetation], in: Reaktorinstitut Graz (Ed.), Tschernobyl-Bericht. Reactor Institute, Graz University of Technology, Graz, pp. 101–114. Available as https://www.researchgate.net/publication/318649309
33. Katzmann W, Schrom H (1986) Umweltreport Österreich [Environmental report Austria]. Kremayr & Scheriau, Vienna.
34. Ahamer G (2019) Mapping Global Dynamics: Geographic Perspectives from Local Pollution to Global Evolution. Springer, Cham. https://doi.org/10.1007/978-3-319-51704-9
35. Currie LA (1968) Limits for qualitative detection and quantitative determination: application to radiochemistry. Anal Chem 40:586–593. https://doi.org/10.1021/ac60259a007
36. ISO (2019) ISO 11929-1:2019. Determination of the characteristic limits (decision threshold, detection limit and limits of the coverage interval) for measurements of ionizing radiation – Fundamentals and application – Part 1: Elementary applications. International Organization for Standardization, Geneva.
37. Limpert E, Stahel WA, Abbt M (2001) Log-normal distributions across the sciences: keys and clues. BioScience 51:341–352. https://doi.org/10.1641/0006-3568(2001)051[0341:LNDATS]2.0.CO;2
38. Spearman C (1904) The proof and measurement of association between two things. Am J Psychol 15:72–101. https://doi.org/10.2307/1412159
39. Efron B, Tibshirani RJ (1993) An Introduction to the Bootstrap. Chapman & Hall, New York. https://doi.org/10.1007/978-1-4899-4541-9
40. Sen PK (1968) Estimates of the regression coefficient based on Kendall's tau. J Am Stat Assoc 63:1379–1389. https://doi.org/10.1080/01621459.1968.10480934
41. Tobin J (1958) Estimation of relationships for limited dependent variables. Econometrica 26:24–36. https://doi.org/10.2307/1907382
42. Helsel DR (2012) Statistics for Censored Environmental Data Using Minitab and R, 2nd ed. John Wiley & Sons, Hoboken. https://doi.org/10.1002/9781118162729
43. Pearson K (1897) Mathematical contributions to the theory of evolution. – On a form of spurious correlation which may arise when indices are used in the measurement of organs. Proc R Soc Lond 60:489–498. https://doi.org/10.1098/rspl.1896.0076
44. Kronmal RA (1993) Spurious correlation and the fallacy of the ratio standard revisited. J R Stat Soc Ser A Stat Soc 156:379–392. https://doi.org/10.2307/2983064

45. McGee EJ, Johanson KJ, Keatinge MJ, Synnott HJ, Colgan PA (1996) An evaluation of ratio systems in radioecological studies. Health Phys 70:215–221. https://doi.org/10.1097/00004032-199602000-00009
46. Fuller WA (1987) Measurement Error Models. John Wiley & Sons, New York. https://doi.org/10.1002/9780470316665
47. Carroll RJ, Ruppert D, Stefanski LA, Crainiceanu CM (2006) Measurement Error in Nonlinear Models: A Modern Perspective, 2nd ed. Chapman & Hall/CRC, Boca Raton. https://doi.org/10.1201/9781420010138
48. Cook JR, Stefanski LA (1994) Simulation-extrapolation estimation in parametric measurement error models. J Am Stat Assoc 89:1314–1328. https://doi.org/10.1080/01621459.1994.10476871
49. Meisel S, Graller P, Kahr G, Ninaus W (1989) Activity in local batches of soil layers, in: Proceedings of the XIX Annual Meeting of the European Society for New Methods in Agricultural Research (ESNA), Vienna, 29 August – 2 September 1988. Report OEFZS-4489, Austrian Research Centre Seibersdorf, pp. 143–156.
50. UNSCEAR (2011) Sources and Effects of Ionizing Radiation. UNSCEAR 2008 Report to the General Assembly with Scientific Annexes, Vol. II, Annex D: Health effects due to radiation from the Chernobyl accident. United Nations, New York.
51. Benjamini Y, Hochberg Y (1995) Controlling the false discovery rate: a practical and powerful approach to multiple testing. J R Stat Soc Ser B 57:289–300. https://doi.org/10.1111/j.2517-6161.1995.tb02031.x
52. Flügel HW, Neubauer F (1984) Geologische Karte der Steiermark 1:200 000 [Geological map of Styria]. Geologische Bundesanstalt, Wien.
53. Schuirmann DJ (1987) A comparison of the two one-sided tests procedure and the power approach for assessing the equivalence of average bioavailability. J Pharmacokinet Biopharm 15:657–680. https://doi.org/10.1007/BF01068419
54. Seabold S, Perktold J (2010) Statsmodels: econometric and statistical modeling with Python, in: Proceedings of the 9th Python in Science Conference, Austin, pp. 92–96. https://doi.org/10.25080/Majora-92bf1922-011
55. Comans RNJ, Hockley DE (1992) Kinetics of cesium sorption on illite. Geochim Cosmochim Acta 56:1157–1164. https://doi.org/10.1016/0016-7037(92)90053-L
56. Comans RNJ, Haller M, De Preter P (1991) Sorption of cesium on illite: non-equilibrium behaviour and reversibility. Geochim Cosmochim Acta 55:433–440. https://doi.org/10.1016/0016-7037(91)90002-M
57. de Koning A, Comans RNJ (2004) Reversibility of radiocaesium sorption on illite. Geochim Cosmochim Acta 68:2815–2823. https://doi.org/10.1016/j.gca.2003.12.025
58. Benedicto A, Missana T, Fernández AM (2014) Interlayer collapse affects on cesium adsorption onto illite. Environ Sci Technol 48:4909–4915. https://doi.org/10.1021/es5003346
59. Absalom JP, Young SD, Crout NMJ (1995) Radio-caesium fixation dynamics: measurement in six Cumbrian soils. Eur J Soil Sci 46:461–469. https://doi.org/10.1111/j.1365-2389.1995.tb01342.x
60. Konoplev AV, Bulgakov AA, Popov VE, Hilton J, Comans RNJ (1996) Long-term investigation of ^{137}Cs fixation by soils. Radiat Prot Dosim 64:15–18. https://doi.org/10.1093/oxfordjournals.rpd.a031555
61. Murota K, Saito T, Tanaka S (2016) Desorption kinetics of cesium from Fukushima soils. J Environ Radioact 153:134–140. https://doi.org/10.1016/j.jenvrad.2015.12.013
62. Kamei-Ishikawa N, Uchida S, Tagami K (2008) Distribution coefficients for ^{85}Sr and ^{137}Cs in Japanese agricultural soils and their correlations with soil properties. J Radioanal Nucl Chem 277:433–439. https://doi.org/10.1007/s10967-007-7125-z
63. Gil-García C, Rigol A, Vidal M (2009) New best estimates for radionuclide solid–liquid distribution coefficients in soils, Part 1: radiostrontium and radiocaesium. J Environ Radioact 100:690–696. https://doi.org/10.1016/j.jenvrad.2008.10.003

64. Konoplev A, Golosov V, Laptev G, Nanba K, Onda Y, Takase T, Wakiyama Y, Yoshimura K (2016) Behavior of accidentally released radiocesium in soil–water environment: looking at Fukushima from a Chernobyl perspective. J Environ Radioact 151:568–578. https://doi.org/10.1016/j.jenvrad.2015.06.019

65. Mukai H, Hirose A, Motai S, Kikuchi R, Tanoi K, Nakanishi TM, Yaita T, Kogure T (2016) Cesium adsorption/desorption behavior of clay minerals considering actual contamination conditions in Fukushima. Sci Rep 6:21543. https://doi.org/10.1038/srep21543

66. Ramírez-Guinart O, Kaplan D, Rigol A, Vidal M (2020) Deriving probabilistic soil distribution coefficients (Kd). Part 2: Reducing caesium Kd uncertainty by accounting for experimental approach and soil properties. J Environ Radioact 223–224:106407. https://doi.org/10.1016/j.jenvrad.2020.106407

67. Elprince AM, Rich CI, Martens DC (1977) Effect of temperature and hydroxy aluminum interlayers on the adsorption of trace radioactive cesium by sediments near water-cooled nuclear reactors. Water Resour Res 13:375–380. https://doi.org/10.1029/WR013i002p00375

68. Baligar VC, Nielsen NE, Barber SA (1979) Kinetics of absorption of K, Rb and Cs from solution culture by intact plant roots. J Plant Nutr 1:25–37. https://doi.org/10.1080/01904167909362697

69. Kaddah MT (1968) Cesium uptake by Sudangrass seedlings from four soils in Southern California. Soil Sci 105:369–375. https://doi.org/10.1097/00010694-196805000-00012

70. Wallace A, Romney EM, Wood RA, Alexander GV (1983) Influence of potassium on uptake and distribution of cesium in bush beans. J Plant Nutr 6:397–403. https://doi.org/10.1080/01904168309363099

71. Shaw G, Bell JNB (1991) Competitive effects of potassium and ammonium on caesium uptake kinetics in wheat. J Environ Radioact 13:283–296. https://doi.org/10.1016/0265-931X(91)90002-W

72. Tschurlovits M, Streisselberger F (1988) Sr, Cs and K radionuclide equilibrium concentration factors in Danube fish. Kerntechnik 52:39–42. https://doi.org/10.1515/kern-1988-520115

73. Smith JT, Kudelsky AV, Ryabov IN, Hadderingh RH (2000a) Radiocaesium concentration factors of Chernobyl-contaminated fish: a study of the influence of potassium, and "blind" testing of a previously developed model. J Environ Radioact 48:359–369. https://doi.org/10.1016/S0265-931X(99)00089-2

74. Barber DA (1964) Influence of soil organic matter on the entry of caesium-137 into plants. Nature 204:1326–1327. https://doi.org/10.1038/2041326a0

75. Tahir M, Stewart JWB (1975) Effect of organic matter incorporation into soils on ^{137}cesium uptake by wheat plants. Radiat Bot 15:323–328. https://doi.org/10.1016/0033-7560(75)90003-4

76. Konoplev A, Kaminski S, Klemt E, Konopleva I, Miller R, Zibold G (2002) Comparative study of ^{137}Cs partitioning between solid and liquid phases in Lakes Constance, Lugano and Vorsee. J Environ Radioact 58:1–11. https://doi.org/10.1016/S0265-931X(01)00075-3

77. Bunzl K, Schultz W (1985) Distribution coefficients of ^{137}Cs and ^{85}Sr by mixtures of clay and humic material. J Radioanal Nucl Chem 90:23–37. https://doi.org/10.1007/BF02037319

78. Fan QH, Tanaka M, Tanaka K, Sakaguchi A, Takahashi Y (2014) An EXAFS study on the effects of natural organic matter and the expandability of clay minerals on cesium adsorption and mobility. Geochim Cosmochim Acta 135:49–65. https://doi.org/10.1016/j.gca.2014.02.049

79. Ritchie JC, McHenry JR (1978) Fallout Cs-137 in cultivated and noncultivated north central United States watersheds. J Environ Qual 7:40–44. https://doi.org/10.2134/jeq1978.00472425000700010008x

80. Smith JT, Comans RNJ, Ireland DG, Nolan L, Hilton J (2000b) Experimental and in situ study of radiocaesium transfer across the sediment–water interface and mobility in lake sediments. Appl Geochem 15:833–848. https://doi.org/10.1016/S0883-2927(99)00095-5

81. Evans EJ, Dekker AJ (1969) Effect of nitrogen on cesium-137 in soils and its uptake by oat plants. Can J Soil Sci 49:349–355. https://doi.org/10.4141/cjss69-048

82. Funaki H, Tsuji H, Nakanishi T, Yoshimura K, Sakuma K, Hayashi S (2022) Remobilisation of radiocaesium from bottom sediments to water column in reservoirs in Fukushima, Japan. Sci Total Environ 812:152534. https://doi.org/10.1016/j.scitotenv.2021.152534

83. Konoplev AV, Wakiyama Y, Wada T, Golosov VN, Nanba K, Takase T (2018) Radiocesium in ponds in the near zone of Fukushima Dai-ichi NPP. Water Resour 45:589–597. https://doi.org/10.1134/S0097807818040139

84. Bradbury MH, Baeyens B (2000) A generalised sorption model for the concentration dependent uptake of caesium by argillaceous rocks. J Contam Hydrol 42:141–163. https://doi.org/10.1016/S0169-7722(99)00094-7

85. Graham ER, Killion DD (1962) Soil colloids as a factor in the uptake of cobalt, cesium, and strontium by plants. Soil Sci Soc Am Proc 26:545–547. https://doi.org/10.2136/sssaj1962.03615995002600060010x

86. Nishita H, Haug RM, Hamilton M (1968) Influence of minerals on Sr^{90} and Cs^{137} uptake by bean plants. Soil Sci 105:237–243. https://doi.org/10.1097/00010694-196804000-00006

87. Delvaux B, Kruyts N, Cremers A (2000) Rhizospheric mobilization of radiocesium in soils. Environ Sci Technol 34:1489–1493. https://doi.org/10.1021/es990658g

88. Vandebroek L, Van Hees M, Delvaux B, Spaargaren O, Thiry Y, Sweeck L (2012) Relevance of Radiocaesium Interception Potential (RIP) on a worldwide scale to assess soil vulnerability to ^{137}Cs contamination. J Environ Radioact 104:87–93. https://doi.org/10.1016/j.jenvrad.2011.09.002

89. Durrant CB, Begg JD, Kersting AB, Zavarin M (2018) Cesium sorption reversibility and kinetics on illite, montmorillonite, and kaolinite. Sci Total Environ 610–611:511–520. https://doi.org/10.1016/j.scitotenv.2017.08.122

90. Kelly MS, Matthews TE, Pinder JE III (1996) Foliar uptake of ^{137}Cs from the water column by aquatic macrophytes. J Environ Radioact 30:271–280. https://doi.org/10.1016/0265-931X(95)00027-8

91. Pinder JE, Hinton TG, Whicker FW (2006) Foliar uptake of cesium from the water column by aquatic macrophytes. J Environ Radioact 85:23–47. https://doi.org/10.1016/j.jenvrad.2005.05.005

92. Marchyulenene DP, Moteyunene EB, Gudavichene NA, Polikarpov GG (1976) Étude de l'accumulation sélective du césium 137, du strontium 90 et du cérium 144 dans les compartiments cellulaires des Characées. Radioprotection 11:263–270. https://doi.org/10.1051/radiopro/19761104263

93. Ahamer G (2026) Radiocaesium and potassium in plants, sediments, sediment extracts and solutions, and bank soils of 26 Styrian water bodies after Chernobyl, 1987–1988 – original survey database [Data set], version 3. Zenodo. https://doi.org/10.5281/zenodo.23898698

Supplementary Files

This is a list of supplementary files associated with this preprint. Click to download.

- J1cSedCsv4Supplement.docx